

# Potential of carbon uptake and local aerosol production in boreal and hemi-boreal ecosystems across Finland and in Estonia

Piaopiao Ke<sup>1</sup>, Anna Lintunen<sup>1,2</sup>, Pasi Kolari<sup>1</sup>, Annalea Lohila<sup>1,3</sup>, Santeri Tuovinen<sup>1</sup>, Janne Lampilahti<sup>1</sup>, Roseline Thakur<sup>1</sup>, Maija Peltola<sup>1</sup>, Otso Peräkylä<sup>1</sup>, Tuomo Nieminen<sup>1</sup>, Ekaterina Ezhova<sup>1</sup>, Mari Pihlatie<sup>4,5</sup>, Asta Laasonen<sup>1</sup>, Markku Koskinen<sup>4,5</sup>, Helena Rautakoski<sup>3</sup>, Laura Heimsch<sup>3</sup>, Tom Kokkonen<sup>1</sup>, Aki Vähä<sup>1</sup>, Ivan Mammarella<sup>1</sup>, Steffen Noe<sup>6</sup>, Jaana Bäck<sup>2</sup>, Veli-Matti Kerminen<sup>1</sup>, Markku Kulmala<sup>1</sup>

<sup>1</sup> Institute for Atmospheric and Earth System Research (INAR) / Physics, Faculty of Science, University of Helsinki, Helsinki, 00014, Finland

<sup>2</sup> Institute for Atmospheric and Earth System Research (INAR) / Forest Sciences, Faculty of Agriculture and Forestry, University of Helsinki, Helsinki, 00014, Finland

<sup>3</sup> Finnish Meteorological Institute, Finland

<sup>4</sup> Department of Agricultural Sciences, Faculty of Agriculture and Forestry, University of Helsinki, Helsinki 00790, Finland

<sup>5</sup> Department of Agricultural Sciences, Faculty of Agriculture and Forestry, University of Helsinki, Helsinki 00790, Finland

<sup>6</sup> Institute of Forestry and Engineering, Estonian University of Life Sciences, 51006 Tartu, Estonia

Correspondence: Markku Kulmala ([markku.kulmala@helsinki.fi](mailto:markku.kulmala@helsinki.fi)) and Piaopiao Ke ([piaopiao.ke@helsinki.fi](mailto:piaopiao.ke@helsinki.fi))

**Abstract:** Continental ecosystems play an important role in carbon dioxide (CO<sub>2</sub>) uptake and aerosol production, which helps to mitigate climate change. The concept of ‘CarbonSink+ potential’ enables a direct comparison of CO<sub>2</sub> uptake and local aerosol production at ecosystem scale. Following this concept, momentary net ecosystem exchange (NEE) and number concentration of negative intermediate ions at 2.0-2.3 nm ( $N_{\text{neg}}$ ) were analysed for boreal and hemi-boreal ecosystems across Finland and in Estonia.  $N_{\text{neg}}$  can tell us how effectively gaseous precursors associated with biogenic emissions from an ecosystem initiate the new particle formation. Four forests, three agricultural fields, an open peatland, an urban garden, and a coastal site were included focusing on summertime. We compared the NEE and  $N_{\text{neg}}$  at each site to the boreal Hyytiälä forest (F-HYY) as it is the dominant ecosystem type in Finland.  $N_{\text{neg}}$  was highest at the urban garden and lowest at the coastal site. The agricultural fields had higher or similar net CO<sub>2</sub> uptake rate and higher  $N_{\text{neg}}$  than all studied forests. The median net CO<sub>2</sub> uptake rate of the open peatland was only 31% of that in F-HYY, while the median  $N_{\text{neg}}$  was 77% of that in F-HYY. The median net CO<sub>2</sub> uptake rate in the urban garden was 63% of that in F-HYY, implying the importance of urban green areas in CO<sub>2</sub> storage. The coastal site was a minor CO<sub>2</sub> sink. Considering the combined effect of CO<sub>2</sub> uptake and aerosol formation and the large area of forests in Finland, the forests are the most important ecosystems helping to mitigate climate warming.

## 1. Introduction

Carbon dioxide (CO<sub>2</sub>) is one of the most abundant greenhouse gases in the atmosphere and the most important cause of global warming (e.g. Jia et al., 2022). Terrestrial ecosystems have an essential role in the global CO<sub>2</sub> budget through carbon uptake from the atmosphere by photosynthesis and its consequent sequestration to various pools (Walker et al., 2021; Friedlingstein et al., 2022). Globally, the net terrestrial ecosystem uptake of CO<sub>2</sub> (i.e. the net carbon sink) is 3.1 Gt C yr<sup>-1</sup>, which accounts for 32% of CO<sub>2</sub> emissions from fossil fuel combustion (Friedlingstein et al., 2022). Terrestrial carbon sequestration, i.e., the process of storing carbon in a carbon pool (IPCC 2022), takes place in both belowground carbon storages (Walker et al., 2021; and the reference therein). Belowground storage includes soil carbon pools, while aboveground storage is primarily in biomass. As a transition between land and open ocean, the coastal environment is identified as an import carbon sink and estimated to uptake 0.4 Gt C yr<sup>-1</sup> (Regnier

et al., 2022). Large spatiotemporal variation of continental CO<sub>2</sub> uptake is assumed due to different ecosystem and land-use types, climatic conditions, and management pathways (Chang et al., 2021; Friedlingstein et al., 2022). The challenge of increasing the carbon sequestration of ecosystems has been attracting more and more attention with the global goal of reducing CO<sub>2</sub> concentrations in the atmosphere.

Apart from acting as CO<sub>2</sub> sinks, terrestrial ecosystems can influence climate by contributing to the formation of new aerosol particles (Kulmala et al., 2004; Kulmala et al., 2014; Kulmala et al., 2020; Yli-Juuti et al., 2021; Junninen et al., 2022; Petäjä et al., 2022, Rätty et al., 2023). Globally, aerosols have been reported to induce a net climate cooling effect. The best estimate of the effective radiative forcing is  $-1.06 \text{ W m}^{-2}$  (Jia et al., 2022). However, large uncertainties exist in the aerosol net radiative forcing estimation, which is tightly associated with the large spatiotemporal heterogeneity in their origin, number concentration and chemical properties.

Atmospheric new particle formation (NPF) is an important source of cloud condensation nuclei (CCN) (e.g. Gordon et al., 2017; Ren et al., 2021; Zhang et al., 2023), which significantly contributes to aerosol-cloud and aerosol-radiation interaction (Rosenfeld et al., 2014; Ezhova et al., 2018, Artaxo et al., 2022; Petäjä et al., 2022). NPF takes place frequently in many environments, such as forests, urban cities, and coastal areas (e.g. Kerminen et al., 2018; Nieminen et al., 2018; Zheng et al., 2021). It has been reported that NPF is greatly enhanced due to the emission of biogenic volatile organic compounds (BVOCs) in boreal forests and peatlands (Junninen et al., 2022; Petäjä et al., 2022). Notably, NPF events often take place regionally, extending over distances up to over 1000 kilometres (Kerminen et al., 2018). Multiple types of ecosystems may contribute to the NPF events in a region depending, for example, on the diversity of land use types. It remains unclear whether and how various ecosystems differ in their contributions to regional NPF, and what is the magnitude of such differences.

To overcome the challenge of analysing the role of local ecosystems in regional aerosol formation, the concept of ‘CarbonSink+ potential’ was recently established (Kulmala et al., 2024). The CarbonSink+ potential enables a direct, ecosystem-scale comparison of CO<sub>2</sub> uptake and the intensity of local intermediate ion formation (LIIF) in the atmosphere at the ecosystem scale. The LIIF can be approximated as the number concentration of negative intermediate ions in 2.0-2.3 nm size range (Tuovinen et al., 2024), to which the aerosol formation at 3-6 nm size range is proportional (Kulmala et al., 2024). The survival probability of small aerosol particles, which

describes the probability of a single particle growing to a certain size without being scavenged, is generally high for particles from 6 nm to CCN size in rural and remote environments (Kulmala et al., 2024; Stolzenburg et al., 2023). The local contributions of certain ecosystems to regional aerosol formation can thus be quantified by LIIF.

This study utilized 1 to 10 year-long datasets of intermediate ion concentrations and CO<sub>2</sub> fluxes from various boreal and hemi-boreal ecosystems across Finland and in Estonia. In summary, four forests, one open peatland, three agricultural fields, one urban garden, and one coastal site were investigated. The negative intermediate ion concentrations and CO<sub>2</sub> fluxes for these ecosystems were compared in different seasons with a focus on the summer. Based on the CarbonSink+ potential concept (Kulmala et al., 2024), the potential of these ecosystems to mitigate climate warming regarding CO<sub>2</sub> uptake and aerosol production is discussed.

## 2. Method

### 2.1 Site description

In this study, various ecosystem types, including forests, open peatland, agricultural fields, coastal area, and an urban garden were studied (Figure 1; Table 1). All stations are utilizing the SMEAR (Station for Measuring Ecosystem-Atmosphere Relations; Hari and Kulmala, 2005) concept. The detailed location, ecosystem type, meteorological characteristics and soil type for each site are presented in Table 1. The SMEAR I in Värriö in northern Finland (F-VAR) and SMEAR II in Hyytiälä in southern Finland (F-HYY) are forest sites both dominated by Scots pine (Kulmala et al., 2019; Neeffjes et al., 2022), while the forests in Ränskälänkorpi (F-RAN) and SMEAR Estonia at Järvelja (F-JAR) are mixtures of coniferous and broadleaf trees (Table 1). While F-VAR and F-HYY are upland forests, i.e., growing on mineral soil, F-RAN is a drained-peatland forest (Laurila et al., 2021) and F-JAR has a mosaic of drained swamp, drained peat, and leached gleyic pseudo-podzols (Kangur et al., 2021; Noe et al., 2015). Two of the agricultural (SMEAR-Agri) sites, i.e. Haltiala (A-HAL), a cereal cropland and Viikki (A-VII), a managed grassland which was renewed in 2023 with a cereal crop (Pihlatie et al., in preparation), are located in Helsinki. The third agricultural site, Qvidja (A-QVI), is a managed grassland located in southwest Finland (Heimsch et al., 2021). The SMEAR II site at Siikaneva (P-SII) is an open, pristine peatland site ~5 km southwest from F-HYY (Rinne et al., 2018). The SMEAR III at Kumpula, Helsinki is an

urban background site. The University of Helsinki botanical garden, and the city of Helsinki allotment garden are in the southwest of SMEAR III station, characterized by a high fraction of vegetation (G-KUM; Järvi et al., 2012). The coastal site (C-TVA) is in Tvärminne Zoological Station, which is a 600-ha nature reserve at the Gulf of Finland entrance (northern Baltic Sea), southwest Finland (Virtasalo et al., 2023). During the measurement period, the annual mean temperature for these sites ranged between 0.4 and 7.2°C, while the annual precipitation ranged between 500 and 750 mm (Table 1). F-JAR, C-TVA, and A-QVI belong to hemi-boreal ecosystems, while the other ecosystems are boreal (Mäki et al., 2022).

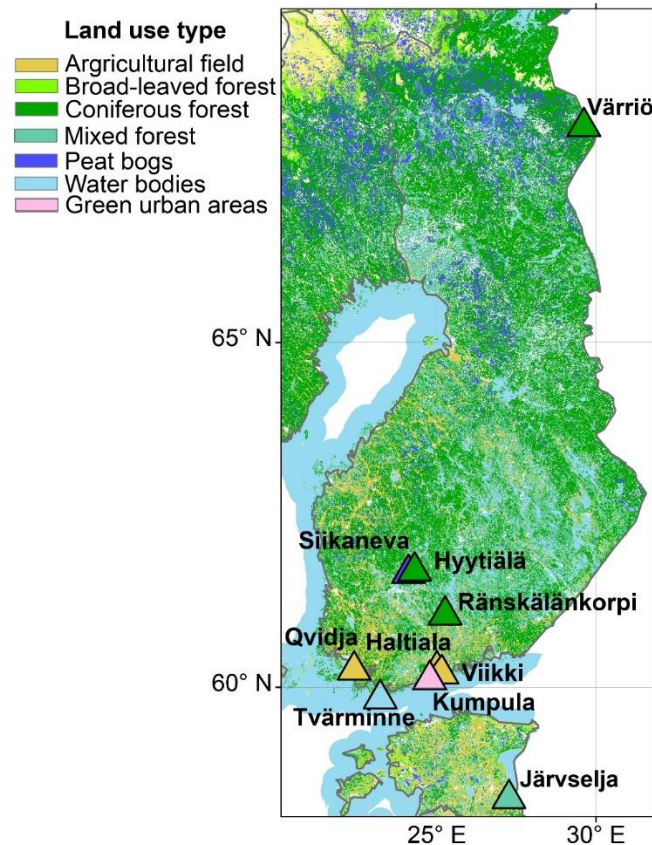


Figure 1. Land type distribution across Finland (Copernicus Land Monitoring Service 2018) and the studied sites with their ecosystem type shown.

Table 1. Meteorological and other main characteristics of the studied sites.

	Sites (Site ID)	Location	Selected period	Mean air tempera- ture (°C)	Rainfall (mm/yr)	Dominant plant species	Peak LAI	Climate Zone
Forest	Hyytiälä, SMEAR II (F-HYY)	61°51'N, 24°17'E	11/2009- 12/2022	4.8	709 <sup>1</sup>	Scots pine and Norway spruce	4.6	Boreal
	Värriö, SMEAR I (F-VAR)	67°46'N, 29°35' E	3/2019- 12/2022	0.4	601 <sup>2</sup>	Scots pine	3.2	Boreal
	Ränskälän korpi (F-RAN)	61°10'N, 25°16'E	4/2021- 12/2022	5.4	600 <sup>3</sup>	Norway spruce, Scots pine, downy birch	----	Boreal
	Järvelja, SMEAR Estonia (F-JAR)	58°16'N, 27°16'E	10/2016- 12/2020	6.8	500-750 <sup>4</sup>	Birch spe- cies, Scots pine, Nor- way spruce	6	Hemi- boreal
Agricultural fields	Haltiala, SMEAR Agri (A-HAL)	60°16'N, 24°57'E	6/2021- 10/2022	6.5	700 <sup>5</sup>	Oat	5.5	Boreal
	Qvidja (A- QVI)	60°18'N, 22°24'E	12/2018- 8/2022	7.0	679 <sup>6</sup>	Timothy, meadow fes- cue	6.2	Hemi- boreal
	Viikki, SMEAR Agri (A-VII)	60°13'N, 25°01'E	7/2022- 6/2023	6.5	792 <sup>5</sup>	Timothy (2022), Bar- ley (2023)	5.2	Boreal
Peatland	Siikaneva, SMEAR II (P-SII)	61°50'N, 24°12'E	11/2019- 12/2022	5.0	710 <sup>7</sup>	Moss and sedges	0.6	Boreal
Urban garden	Kumpula, SMEAR III (G- KUM)	60°12'N, 24°58'E	5/2016- 12/2022	6.3 <sup>5</sup>	731 <sup>5</sup>	Mixed	-----	Boreal
Coastal area	Tvärminne (C-TVA)	59°51'N, 23°15'E	6/2022- 8/2023	7.2 <sup>5</sup>	639 <sup>5</sup>	Seagrass and seaweed	----	Hemi- boreal

<sup>1</sup> Neefjes et al. (2022); <sup>2</sup> Kulmala et al. (2019); <sup>3</sup> Laurila et al. (2021); <sup>4</sup> Noe et al. (2015); <sup>5</sup> Finnish Meteorology Institute, only data at the same calendar year of selected period and same or nearby stations as NAIS and eddy covariance measurements were applied; <sup>6</sup> Heimsch et al. (2021); <sup>7</sup> Rinne et al. (2018); ---- data not available.

## 2.2 Atmospheric measurements: intermediate ions, CO<sub>2</sub> flux, and meteorological parameters

The number concentration of ions and particles and net ecosystem exchange of CO<sub>2</sub> (NEE) were measured using a Neutral cluster and air ion spectrometer (NAIS, Airl Ltd; Mirme and Mirme, 2013) and eddy covariance method (Aubinet et al., 1999), respectively. The meteorological data, e.g., air temperature, air humidity, and photosynthetic photon flux density (PPFD), were measured simultaneously at same heights with the eddy covariance setup. If the meteorological measurement at the same height (Table S1) was not available, it was replaced by the one from the nearest height. The types of analysers and detectors at each site are listed in Table S1.

The NAIS is capable of continuous monitoring of ion and total particle concentrations and size distributions over the diameter range of 0.8-42 nm. The ions can be divided into three different size ranges, namely small ions (also named as cluster ions) in sub-2 nm size range, intermediate ions (2-7 nm), and large ions (>7 nm; Tammet et al., 2014). The time resolution was set to five minutes to optimize signal-to-noise ratio (Mirme and Mirme, 2013). The data were quality-checked, considering e.g. the potential interference of rainfall and snow events on the measurements (Manninen et al., 2016). The ion and total particle number concentration were further averaged over half an hour. The inlets for all the NAIS in all studies sites are 1-2 m high above ground.

In this study, we identified the concentration of negative intermediate ions, specifically within the range of 2.0-2.3 nm ( $N_{\text{neg}}$ ), as an indicator of the local intermediate ion formation (LIIF). It is important to note that the intensity of LIIF can serve as an estimate of the local contribution to the regional NPF (Kulmala et al., 2024). It has been observed that  $N_{\text{neg}}$  displays distinct difference between new particle formation and non-formation periods of intermediate ions (2-7 nm; Tuovinen et al., 2024), thereby making  $N_{\text{neg}}$  a reliable indicator of LIIF. Moreover, the measurement of negative intermediate ions between 2.0 and 2.3 nm by NAIS provides a relatively high degree of accuracy, and their footprints are constrained within the ecosystem scale when measured under the canopy (sub-1 km; Tuovinen et al., 2024; Kulmala et al., 2024). Moreover, the median values of  $N_{\text{neg}}$  between 00:00 and 06:00, i.e. outside the active hours of the ecosystem, were taken as the background concentration at each site. The background value of  $N_{\text{neg}}$  was calculated separately for each season. A narrower time window for background concentration compared to the one proposed by Aliaga et al. (2023), 21:00-06:00, was applied due to the more northern F-VAR with longer day length in the summer in this study. We then

calculated the changes of  $N_{\text{neg}}$  ( $\Delta N_{\text{neg}}$ ) by subtracting the background concentration in each season from  $N_{\text{neg}}$ . The diurnal variation of median  $\Delta N_{\text{neg}}$  were presented together with  $N_{\text{neg}}$  (Section 3). The use of  $\Delta N_{\text{neg}}$  was assumed to eliminate the influence of background clustering at different sites (Aliaga et al., 2024), so that it reflects the intensity of negative intermediate ion production from the specific ecosystem.

The eddy covariance measurement of  $\text{CO}_2$  fluxes is based on the turbulence theory, i.e. assumption that the turbulent flux remains relatively stable in a constant flux layer above the canopy (Lee and Hu, 2002), and it is equal to the covariance of vertical wind speed and ambient  $\text{CO}_2$  concentration in flat and horizontally homogeneous surface (Aubinet et al., 1999). The fluxes were measured above the ecosystem canopies and below 30 m. The detailed measurement height for each site is listed in Table S1. The measurement system requires a fast-response analyser of the  $\text{CO}_2$  concentration (10 Hz) and 3-D sonic anemometer. The raw eddy covariance 10 Hz-data were pre-processed with standard steps, including despiking, detrending, dilution correction and 2-D coordinate rotation (Aubinet et al., 1999). The fluxes were further lag-time adjusted and corrected for spectral loss (Aubinet et al., 1999). Either EddyUH (Mammarella et al., 2016) or EddyPro (Fratini and Mauder, 2014), or the program introduced by Heimsch et al. (2021) were applied for the pre-processing for one site. The processed fluxes were accepted only if they met the stationarity and developed turbulence criterion (Foken and Wichura, 1996) exceeding the site-specific friction velocity thresholds (Table S1). The quality-checked  $\text{CO}_2$  fluxes at the forest sites were further partitioned into gross primary production (GPP) and ecosystem respiration ( $R$ ) using site-specific dependence of  $R$  on the air and/or soil temperature and GPP on the PPFD and air and/or soil temperature (Kulmala et al., 2019).

### 2.3 Data selection criteria

In this study, the analyses were restricted to periods when both negative intermediate ion concentration and NEE were available (Table 1). Therefore, different time periods were applied for each of different sites. For F-HYY, F-VAR, F-JAR, F-QVI, P-SII, and G-KUM, the long-term data were available for more than 3 years. At F-HYY, 12 years of continuous observations were used. For the sites with recently established atmospheric measurement, C-TVA, F-RAN, A-HAL and A-VII - data were available for approximately 1 to 1.5 years. In total, 35 site-years of data were utilized in this study. As we focused on the potential of the ecosystem to uptake  $\text{CO}_2$  and form intermediate ions, the inter-annual variation at the sites was not discussed in this study (Kulmala et al., 2019; Alekseychik et al., 2021; Heimsch et al., 2021).



F-HYY had the longest data recordings (Table 1) among the ten sites and received relatively little anthropogenic pollution (Neefjes et al., 2022). Due to the thinning of F-HYY in the beginning of year 2020, when 40% of tree basal area was removed (Aalto et al., 2023), data from that year were discarded from the analyses to exclude the immediate thinning effect on the studied variables. In F-RAN, the western part of the site was selectively harvested (~60% of basal area removed) and the eastern part of the site was clear-cut in the spring and summer of 2021 with control site left in the middle. The NAIS equipment was positioned in the border between the control and clear-out, ~230 m east from the eddy covariance tower (measurement height of 29 m). The eddy covariance tower was in the border between control and selective harvested plots. In this study, only data with wind blowing from the area after selective harvesting from the west ( $WD > 180^\circ$ ) and wind speed above  $2 \text{ m s}^{-1}$ , were considered. Note that carbon removed from the site in harvested tree biomass is not accounted in the measured flux of  $\text{CO}_2$ . At G-KUM, data from the garden area, i.e.,  $180^\circ$ - $320^\circ$ , were applied. The vegetation varied largely from broadleaf forests to gardens (Järvi et al., 2012).

At the agricultural sites, the management activity is relatively intense and can distinctly influence the  $\text{CO}_2$  fluxes (Heimsch et al., 2021). Note that the carbon removed in harvested crop biomass and the carbon added to the site in fertilizers do not directly contribute to the measured net flux of  $\text{CO}_2$ . For A-QVI, NAIS and eddy covariance data from wind directions from  $30$  to  $140^\circ$  were discarded due to another separated experimental plot located in that part of the field (Heimsch et al., 2021). Also, the data were discarded when the flux footprint was not sufficiently representative of the target grassland (Heimsch et al., 2021). Similarly, at A-VII, only measurements from wind direction between  $145^\circ$  and  $245^\circ$  were included in the analysis to avoid data from other nearby fields with different vegetation and management activities. A-QVI was harvest in June and August, A-VII was harvested twice in August during the reported period, and A-HAL was harvested once only at the end of the growing season during the measurement periods. The sowing (over-seeding for A-QVI and only in 2022) and first-fertilization in the year usually takes place in the end of spring.

The open peatland at P-SII is surrounded by forests. However, 80% of the  $\text{CO}_2$  flux footprint is within ~150 m from the measurement tower, i.e., constrained within the peatland (Alekseychik et al., 2021). At C-TVA, the NAIS instrument trailer is on the shore, and the eddy covariance mast is on an island, ~110 m east of the shore. Only data with wind direction from  $95^\circ$  to  $165^\circ$  and from  $205^\circ$  to  $240^\circ$ , i.e., from the coastal water without being disturbed by trees on nearby islands, were included in the analysis at this site.

### 3. Results and discussion

#### 3.1 Comparison of momentary NEE in different ecosystems

The diurnal variation of NEE between the studied forests, urban garden area, agricultural fields, open peatland, and coastal site in spring (MAM) and summer (JJA) are presented in Figures 2-4. The corresponding comparison in the autumn (SON) and winter (DJF) are presented in Figures S1-S3.

For the forest sites, the hemi-boreal F-JAR tended to have the highest net CO<sub>2</sub> uptake rate (absolute values of NEE when it is negative) at midday (10:00-14:00) in both spring and summer. The median net CO<sub>2</sub> uptake rate at midday in F-JAR reached 12  $\mu\text{mol m}^{-2} \text{s}^{-1}$  in summer. The lowest net CO<sub>2</sub> uptake rate at midday was found in the most north F-VAR, with the median being 4.69  $\mu\text{mol m}^{-2} \text{s}^{-1}$ . This difference may be due to the air temperature 6-8°C higher in the hemi-boreal Estonian forest and lower temperature at F-VAR (Figure S4), as the ecosystem productivity at high latitudes in Europe is typically temperature limited (Yi et al., 2010).

In summer, the net CO<sub>2</sub> uptake rate in the urban garden area at G-KUM was comparable with the drained peatland forest F-RAN. The vegetation fraction in G-KUM is relatively high (0.44). During summertime, the strong photosynthesis dominated the changes of CO<sub>2</sub> fluxes, inducing a net CO<sub>2</sub> uptake in the garden section (Järvi et al., 2012). In the other seasons, the urban garden area was a net source of CO<sub>2</sub> most of the time (Figures 2 and S1), similar to the results previously reported for the years 2006-2010 from the same site (Järvi et al., 2012). There are residential buildings and traffic within the eddy covariance measurement footprint in G-KUM. The CO<sub>2</sub> emissions from the residential buildings, traffic and soils outweighed photosynthetic uptake of CO<sub>2</sub> except from the summer daytime.

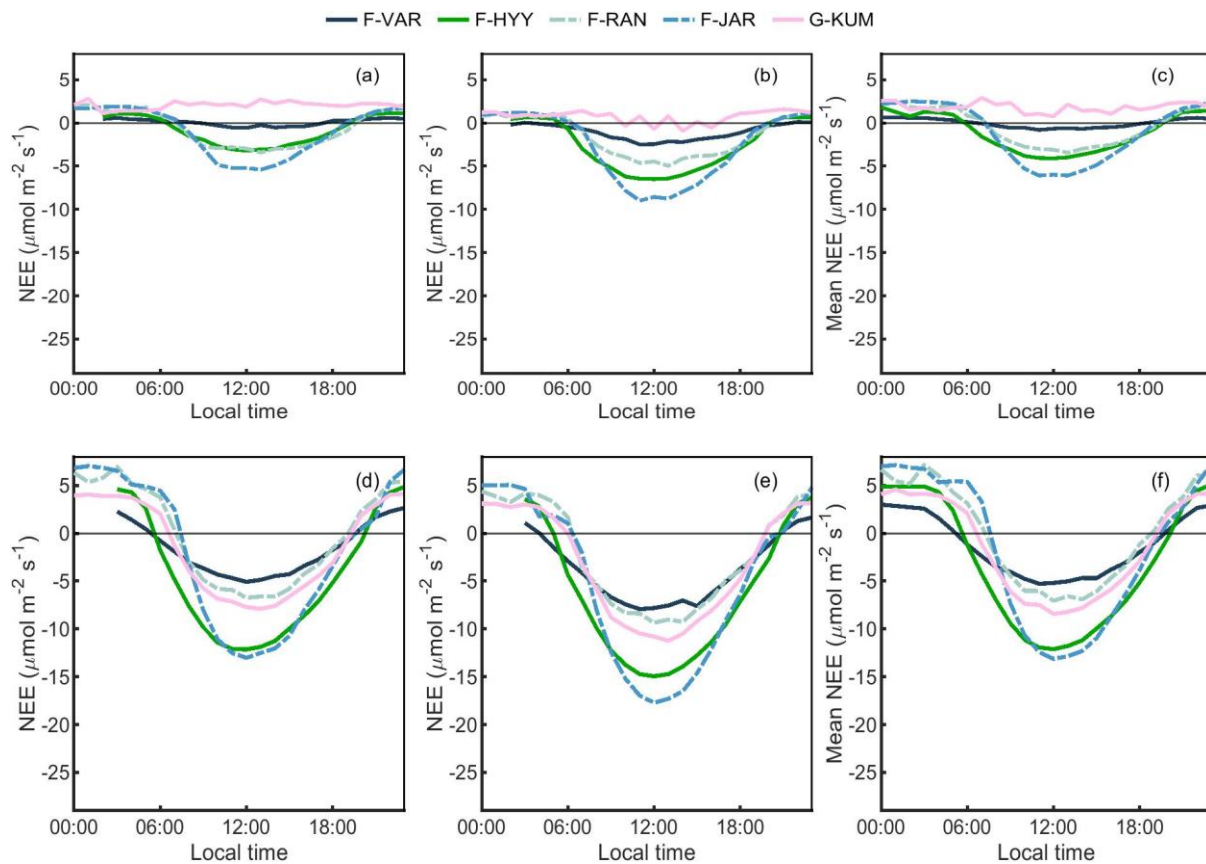


Figure 2. The 50<sup>th</sup> percentile (a), 25<sup>th</sup> percentile (b), and mean values (c) of NEE at each hour  
 255 for the forest sites and urban garden in spring (MAM) and the corresponding 50<sup>th</sup> percentile,  
 25<sup>th</sup> percentile, and mean values in summer (JJA), (d), (e), (f), respectively.

In the case of agricultural fields in summer (Figure 3), the A-HAL and A-VII croplands had 2-  
 5  $\mu\text{mol m}^{-2} \text{s}^{-1}$  (for the median values at midday) higher momentary net CO<sub>2</sub> uptake rate than  
 260 A-VII. Notably, in spring, the croplands in A-VII and A-HAL were net sources of CO<sub>2</sub>, while  
 A-QVI was a CO<sub>2</sub> sink during daytime with a comparable uptake rate to the F-HYY (ranging  
 between 0 and 4  $\mu\text{mol m}^{-2} \text{s}^{-1}$ ). The different plant species (Table 1) and management activities  
 between the agricultural fields likely caused the differences in their seasonal CO<sub>2</sub> fluxes.  
 During the measurement period, perennial grass species were grown in A-QVI, while the  
 265 growth of the annual crops in A-HAL and A-VII relied on the sowing and fertilization date,  
 normally at the end of spring. This may explain the springtime CO<sub>2</sub> emission in A-HAL and  
 A-VII. In the summer, the A-HAL and A-VII was harvested only in August, while A-QVI was  
 harvested in June and August separately, which may explain the higher CO<sub>2</sub> uptake rate in A-  
 Hal and A-VII. The upper quartile of the momentary net CO<sub>2</sub> uptake, i.e., absolute values of

25<sup>th</sup> percentile NEE, was 62% higher in A-HAL than that in F-HYY in summer. The midday momentary net CO<sub>2</sub> uptake rate in A-VII was 17% higher than that in F-HYY, while that in A-QVI was 30% lower than in F-HYY. It is also important to note that the harvests of plant biomass decreased local carbon storage which was not accounted for in the measured CO<sub>2</sub> fluxes. In the studies agricultural fields, the harvest was conducted once or twice every year, whereas the typical rotation length in managed boreal are 60-100 years in Southern Finland.

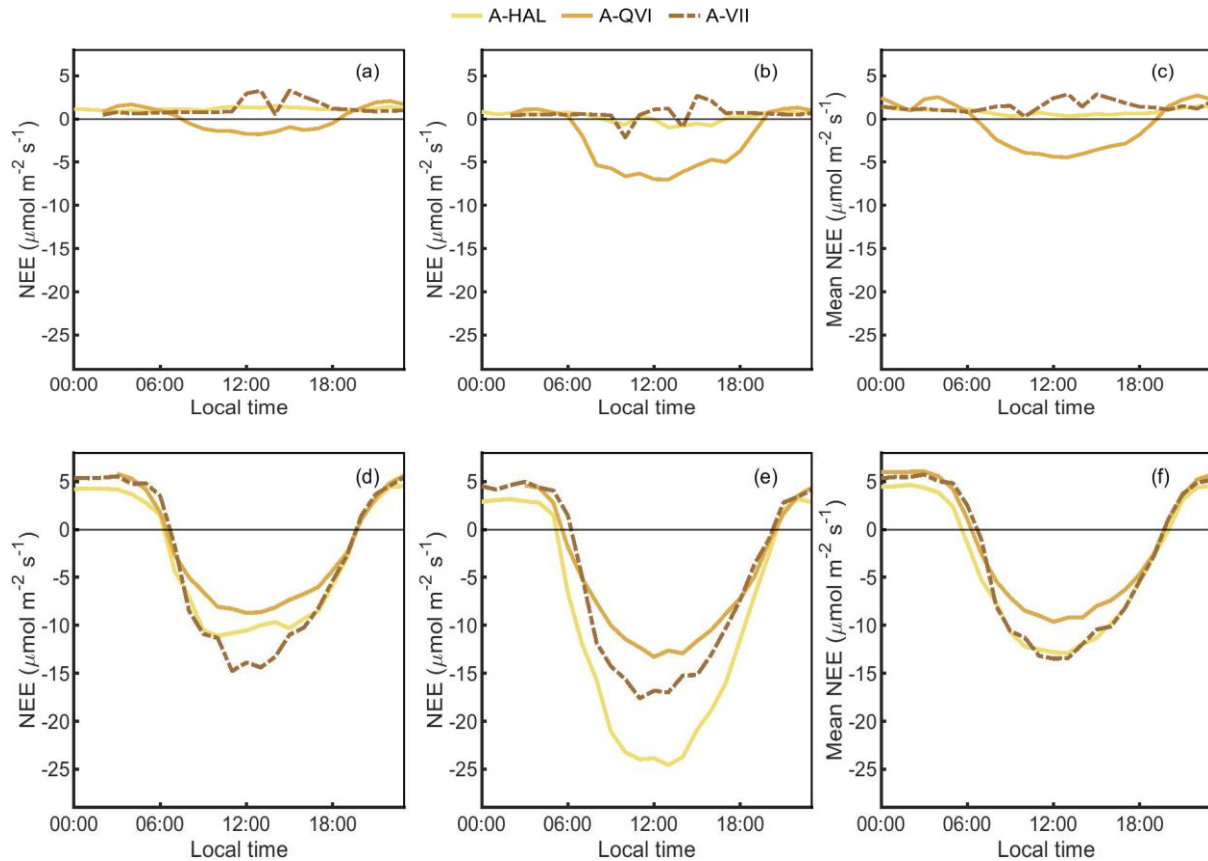


Figure 3. The 50<sup>th</sup> percentile (a), 25<sup>th</sup> percentile (b), and mean values (c) of NEE at each hour for the agricultural fields in spring (MAM) and the corresponding 50<sup>th</sup> percentile, 25<sup>th</sup> percentile, and mean values, (d), (e), (f), in summer (JJA), respectively.

The CO<sub>2</sub> uptake rate and respiration rate (nighttime CO<sub>2</sub> fluxes) in the open peatland (P-SII) and coastal area C-TVA (Figure 4) were distinctly lower than those in the agricultural fields and forests during spring and summer. Still, the P-SII remained a net sink of CO<sub>2</sub> during daytimes in all the seasons except in winter. The midday NEE at C-TVA were -0.25 and -0.01 μmol m<sup>-2</sup> s<sup>-1</sup> in spring and summer, respectively. Hence, stronger net CO<sub>2</sub> uptake possibly appears in spring in this Baltic coastal area under certain conditions, i.e., when the partial

pressure of CO<sub>2</sub> in the water is lower than that in the air (Roth et al., 2023). This may be induced  
 290 by fast growth of phytoplankton and submerged vegetation in the spring (Roth et al., 2023).

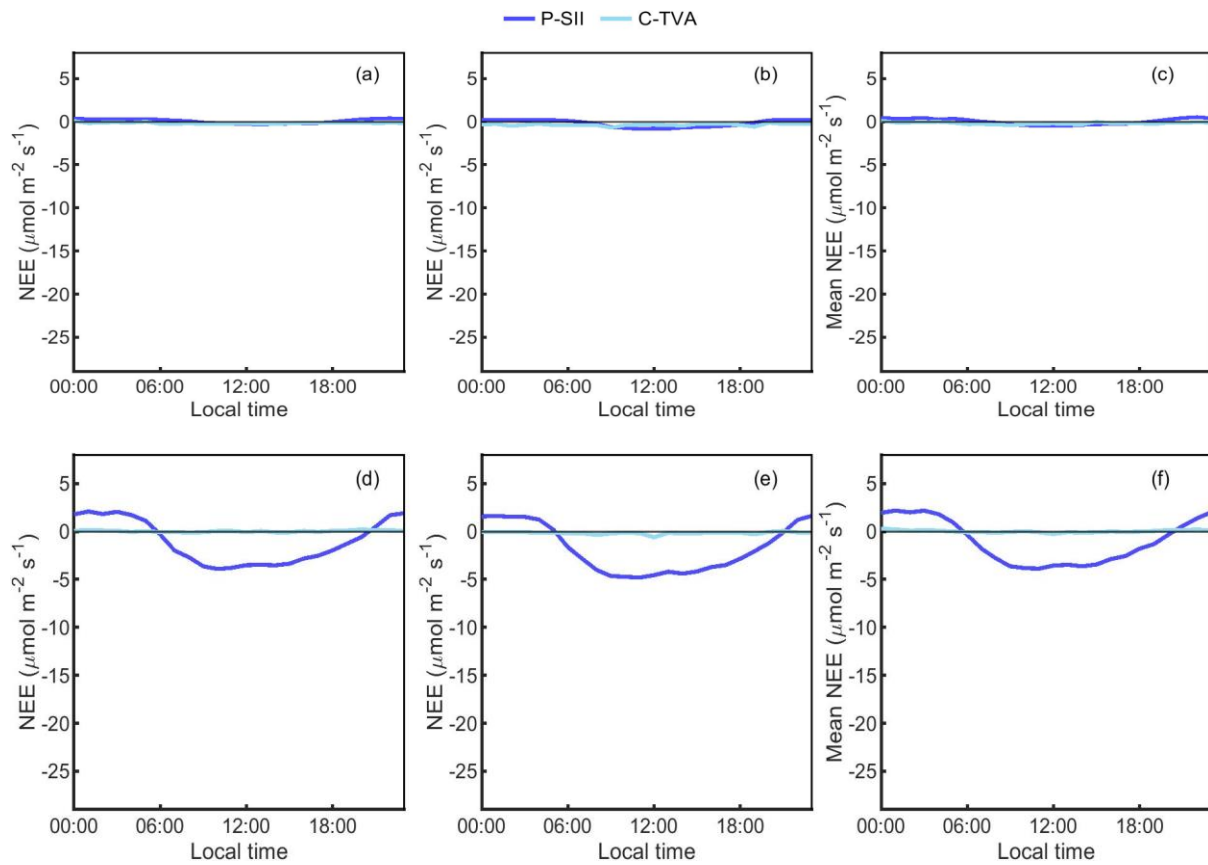


Figure 4. The 50<sup>th</sup> percentile(a), 25<sup>th</sup> percentile (b), and mean values (c) of NEE at each hour  
 295 for the peatland and coastal area in spring (MAM) and the corresponding 50<sup>th</sup> percentile, 25<sup>th</sup>  
 percentile, and mean values in summer (JJA), respectively.

Additionally, the F-RAN and F-JAR turned into a CO<sub>2</sub> source 1-2 hours earlier in the late  
 afternoon of summer than the other two forests (Figure 2). Note that the soil at F-RAN and F-  
 300 JAR is mainly drained peatland and water-logged soil (Table 1), respectively, which is  
 indicated by high organic carbon content (Laurila et al., 2021; Noe et al., 2015). The elevated  
 air temperature (Figure S4) and increased soil organic carbon content may contribute to the  
 enhanced respiration at the two sites, which is reflected in the nighttime fluxes (Figure 2).  
 Hence, even though the GPP at F-JAR and F-RAN in the late afternoon were close to that at  
 305 F-HYY (Figure 5), net emissions of CO<sub>2</sub>, i.e., positive NEE values, were observed at these two  
 forest sites in the earlier and later hours of the day.

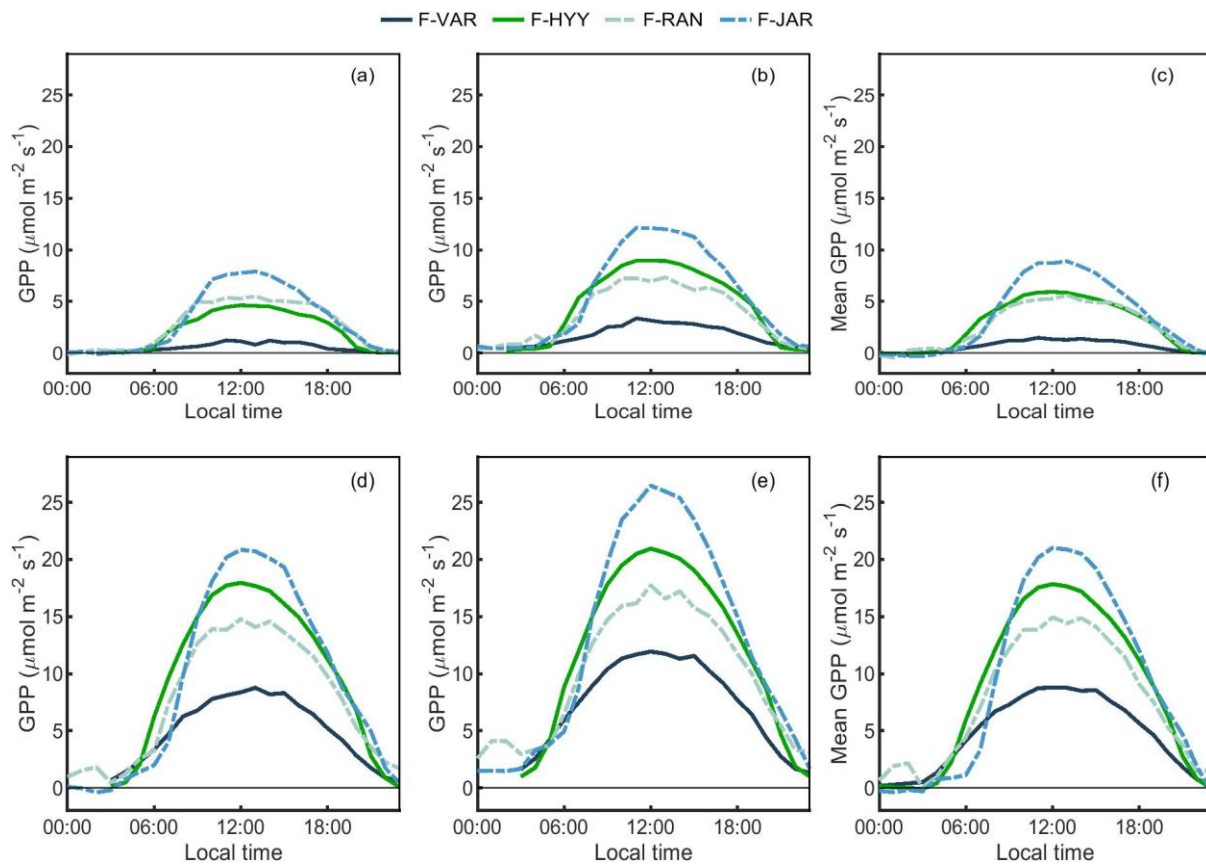


Figure 5. The 50<sup>th</sup> percentile (a), 75<sup>th</sup> percentiles (b), and mean values (c) of GPP at each hour for the forest sites in spring (MAM) and the corresponding 50<sup>th</sup> percentile, 75<sup>th</sup> percentile, and mean values in summer (JJA), (d), (e), (f), respectively.

### 3.2 Comparison of negative intermediate ion concentrations across different ecosystems

The comparison of  $N_{\text{neg}}$  between different ecosystems in spring and summer are presented in Figures 6-8. It was assumed that negative intermediate ions at 2.0-2.3 nm can describe how efficiently the ecosystem can produce new aerosol particles (Kulmala et al., 2024; Tuovinen et al., 2024). The corresponding values of  $N_{\text{neg}}$  in autumn and winter were only 16-84% of those in spring and summer (Figures S5-S7). The  $N_{\text{neg}}$  in the daytime in spring were significantly higher than those in the summer at A-HAL and G-KUM (Mann-Whitney U test based on daily medians,  $P < 0.05$ ). At F-VAR, F-HYY, and F-RAN the median values in summer were significantly higher than those in spring ( $P < 0.05$ ). For other sites, the difference was not significant ( $P > 0.05$ ). In contrast, the difference between 75<sup>th</sup> and 50<sup>th</sup> percentiles of  $N_{\text{neg}}$  in spring was higher than those in summer in all the studied sites except F-VAR and C-TVA. The larger upper quartile deviation of  $N_{\text{neg}}$  in spring implied that the LFII were either more frequent

or stronger in spring than in summer at all the sites except F-VAR and C-TVA (Dada et al., 2018; Nieminen et al., 2018).

For all the sites, the diurnal variation of negative intermediate ions in spring and summer was clear except C-TVA in spring, i.e., a distinct peak in the daytime. In the winter, the diurnal cycle of  $N_{\text{neg}}$  was not visible in any of the studied sites (Figures S6-S8). This agrees with the observation that the global radiation and air temperature are observed to correlate positively with concentration of negative intermediate ions at 2-4 nm in F-HYY (Neeffjes et al., 2022).

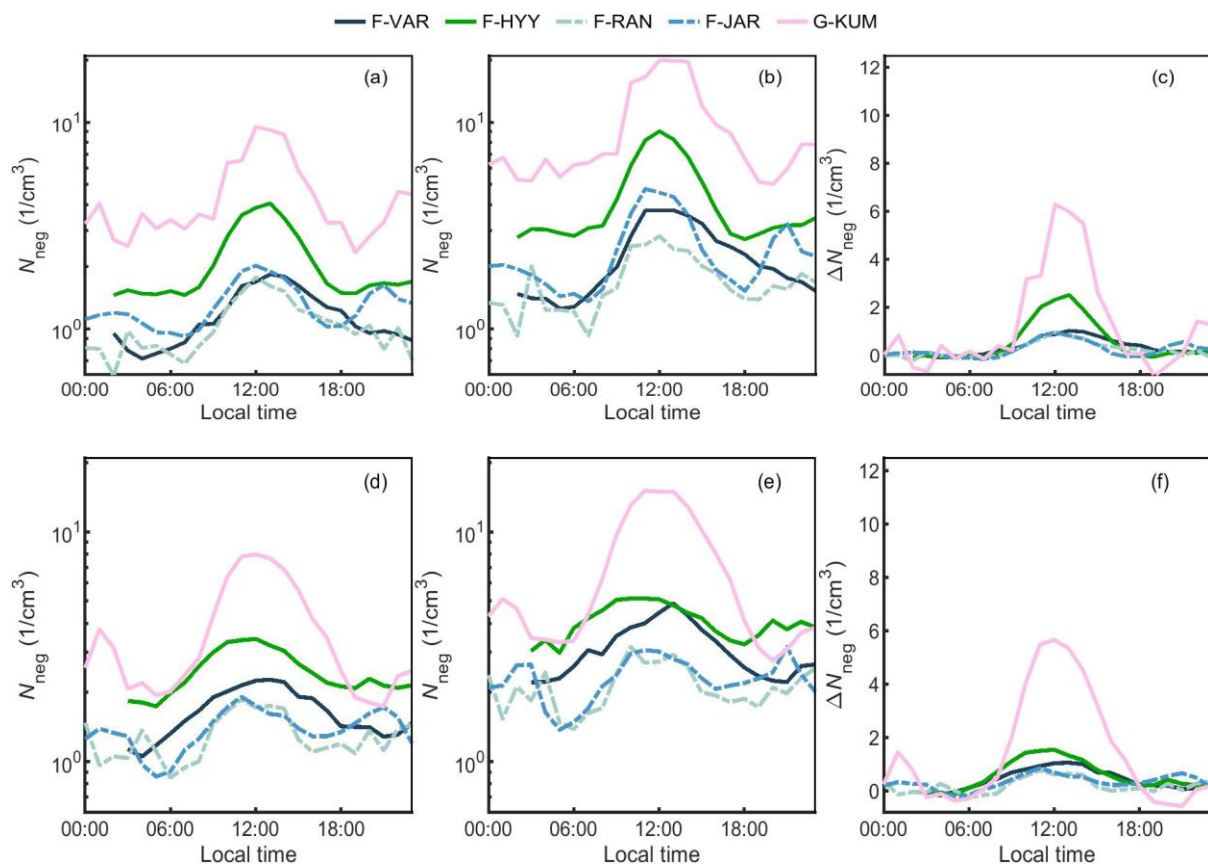


Figure 6. The 50<sup>th</sup> percentile (a) and 75<sup>th</sup> percentile (b) of negative intermediate ions ( $N_{\text{neg}}$ ) at 2.0-2.3 nm ( $N_{\text{neg}}$ ) at each hour and the daily fluctuations of  $N_{\text{neg}}$  (c) for the forests and urban garden in spring (MAM) and the corresponding 50<sup>th</sup> percentile, 75<sup>th</sup> percentile, and normalized concentration for median values in summer (JJA), (d), (e), (f), respectively.



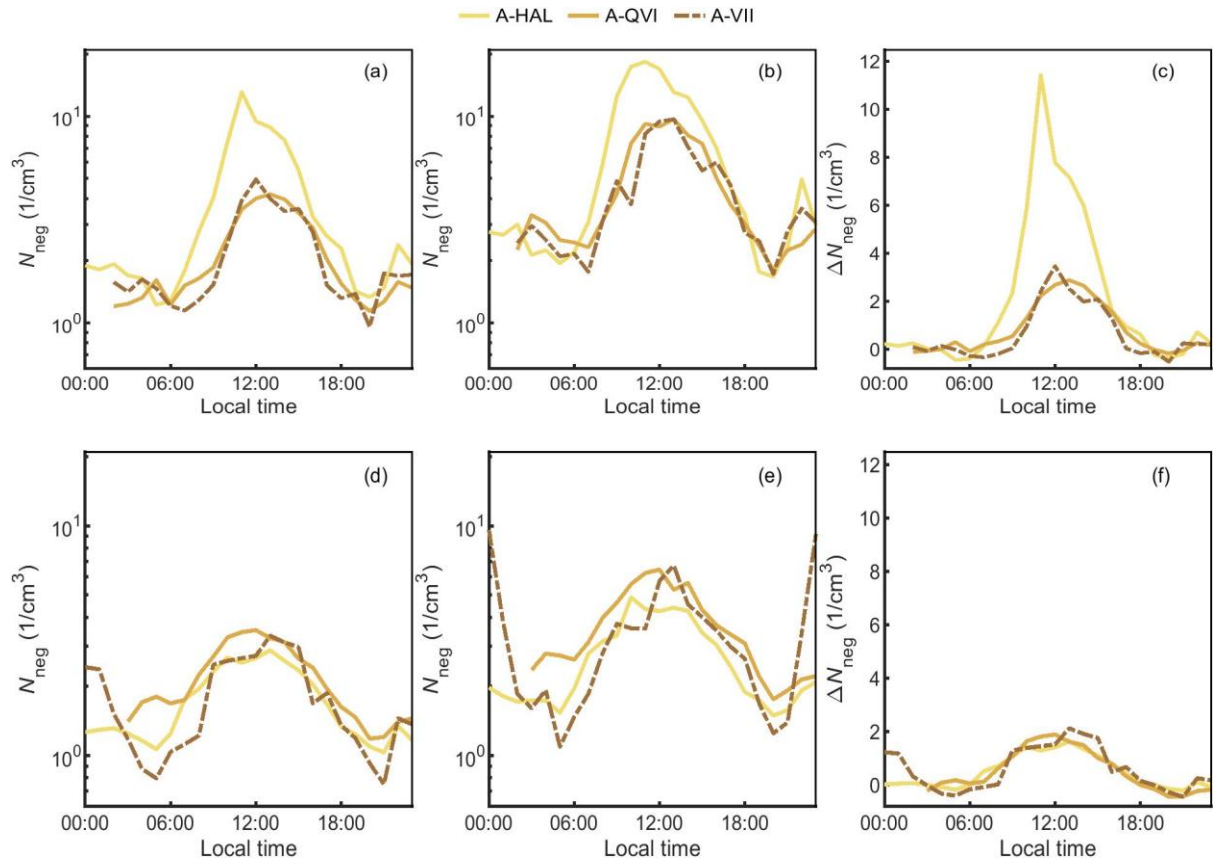


Figure 7. The 50<sup>th</sup> (a) and 75<sup>th</sup> percentile (b) of negative intermediate ions ( $N_{\text{neg}}$ ) at 2.0-2.3 nm at each hour and the daily fluctuations of  $N_{\text{neg}}$  (c) for the agricultural fields in spring (MAM) and the corresponding 50<sup>th</sup> percentile, 75<sup>th</sup> percentile and normalized concentration for median values, (d), (e), (f), in summer (JJA), respectively.



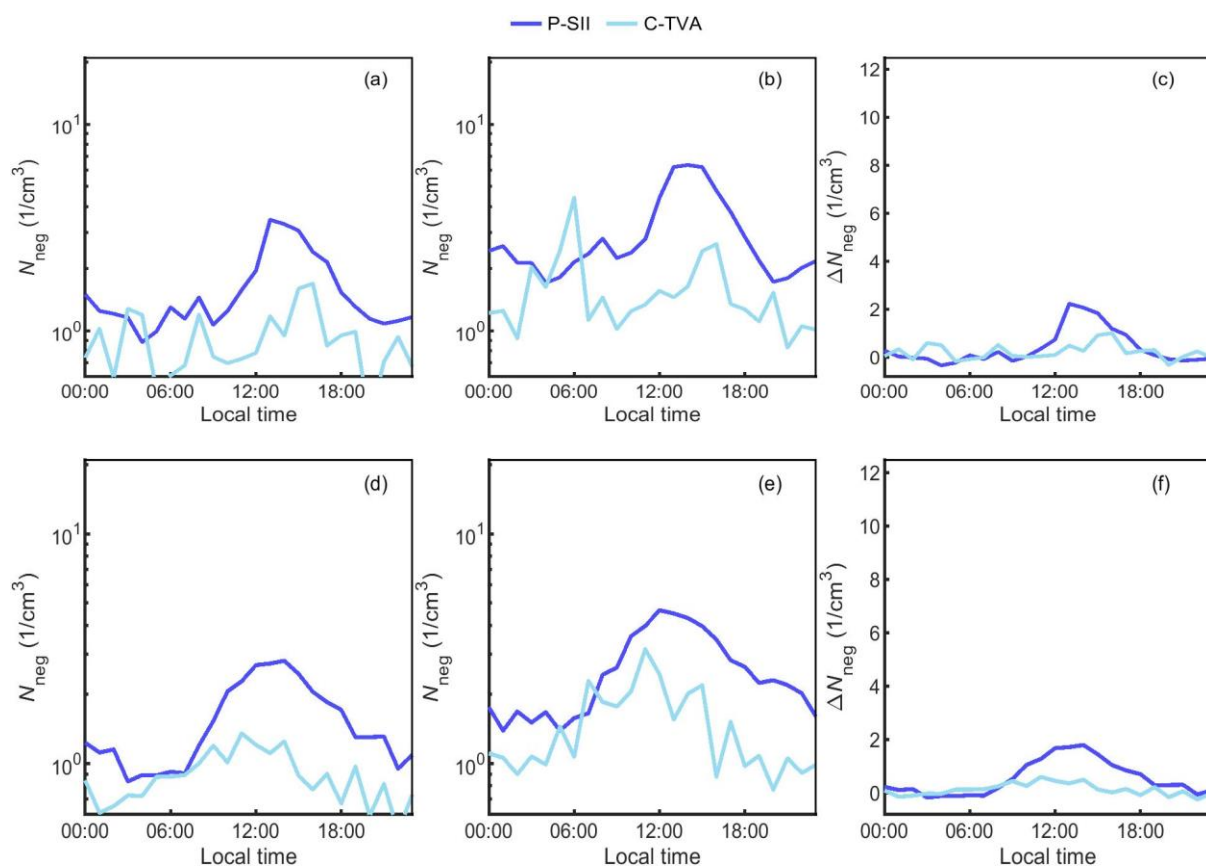


Figure 8. The 50<sup>th</sup> percentile (a) and 75<sup>th</sup> percentile (b) of negative intermediate ions ( $N_{\text{neg}}$ ) at 2.0-2.3 nm at each hour and the daily fluctuations of  $N_{\text{neg}}$  (c) for the peatland and coastal area in spring (MAM) and the corresponding 50<sup>th</sup> percentile, 75<sup>th</sup> percentile, and normalized concentration for median values in summer (JJA), (d), (e), (f), respectively.

The daily fluctuations of  $N_{\text{neg}}$  ( $\Delta N_{\text{neg}}$ ) were calculated by subtracting the background concentration from  $N_{\text{neg}}$  in each season (Section 2.2). In spring, median  $\Delta N_{\text{neg}}$  in the midday for the forests ranged between 0.8 and 2.0  $\text{cm}^{-3}$  (Table S2), with the lowest value in F-JAR and the highest value in F-HYY. The midday mean  $\Delta N_{\text{neg}}$  at the G-KUM was 4.9  $\text{cm}^{-3}$ , which was 2-7 times of that in the studied forests. The presence of more abundant nucleation precursors at the G-KUM may facilitate the ion formation (Nieminen et al., 2018). Seasonal changes in the clustering precursors and their dependence on air temperature and radiation may drive the seasonal variation of  $\Delta N_{\text{neg}}$  at all the sites.

It is notable that generally the agricultural sites had higher midday  $\Delta N_{\text{neg}}$  than the forest sites in spring, varying between 2.3 and 7.7  $\text{cm}^{-3}$ . The application of fertilizers is known to remarkably increase the atmospheric concentration of ammonia ( $\text{NH}_3$ ) in agricultural fields,

e.g., observed in A-QVI (Olin et al., 2022).  $\text{NH}_3$  can stabilize the critical clusters in the nucleation process driven by sulfuric acid ( $\text{H}_2\text{SO}_4$ ).  $\text{H}_2\text{SO}_4$  in the air is majorly formed by oxidation of sulphur dioxide, which can be transported from a longer range than the intermediate ions. However, the frequency of NPF events was found not to increase after the fertilization in A-QVI (Dada et al., 2023). Similarly, the frequency of daytime NPF events did not correlate with agriculture activities in a cropland in France (Kammer et al., 2023). Dada et al. (2023) observed that  $\text{NH}_3$ ,  $\text{H}_2\text{SO}_4$ , and low volatile organic compounds originating from BVOC oxidation play a synergistic role in clustering in A-QVI, resulting in a 7-57 and 2-16 times higher formation rate and number concentration of particles than in F-HYY, respectively. Note that since the A-HAL and A-VII croplands are located in Helsinki, the nucleation precursors and thereby the nucleation rate may be enhanced by anthropogenic pollution in the city. The exact reasons why there were higher  $N_{\text{neg}}$  and  $\Delta N_{\text{neg}}$  at these agricultural sites require more measurement of the clustering precursors.

Furthermore, in spring and summer, the night-time  $N_{\text{neg}}$  increased again at around 20:00 for all the sites, suggesting a ubiquitous nighttime clustering in warm seasons (Mazon et al., 2016). However, these nighttime clustered negative ions are likely unable to grow  $>3$  nm in diameter (Mazon et al., 2016). Moreover, in summer, the 75<sup>th</sup> percentile of nighttime  $N_{\text{neg}}$  at A-VII was comparable with the daytime  $N_{\text{neg}}$ . The decreased boundary layer height (Chen et al., 2016; Neefjes et al., 2022), especially in clear nights, may also facilitate the accumulation of formed clusters and eventually lead to the nighttime peak.

### 3.3 Potential of different ecosystems to contribute to $\text{CO}_2$ uptake and negative intermediate ion production

Since we aimed to compare the potential of ecosystems for net  $\text{CO}_2$  uptake and local production of negative intermediate ions (LIIF), the most active periods for the ecosystem plants are discussed in detail in this section, i.e., midday in summertime. The potential of the studied ecosystems for net  $\text{CO}_2$  uptake and LIIF at midday during summertime are listed in Table 2. The value of NEE and  $N_{\text{neg}}$  at F-HYY were also used as references, to which NEE and  $N_{\text{neg}}$  at all other sites were compared (Table 2). For median values in summer,  $N_{\text{neg}}$  was found to be highest in the urban garden, followed by the agricultural fields (Figure 9). The agricultural fields generally had higher  $N_{\text{neg}}$  than the studied forests and the open peatland (P-SII) had 23% lower  $N_{\text{neg}}$  than F-HYY but 15-46% higher than the other forests. The  $N_{\text{neg}}$  at the coastal area was the lowest. The momentary net  $\text{CO}_2$  uptake rate at midday in summer was highest in

agricultural fields, followed by the forests. The urban garden in this study displayed distinct  
400 net CO<sub>2</sub> uptake, 37% lower than the forests and ~2 times that in the open peatland. The coastal  
area at midday in summer was a very weak CO<sub>2</sub> sink. In the urban garden area in G-KUM,  
median  $N_{\text{neg}}$  was double that in F-HYY, while the median NEE only reached 63% of that in F-  
HYY.

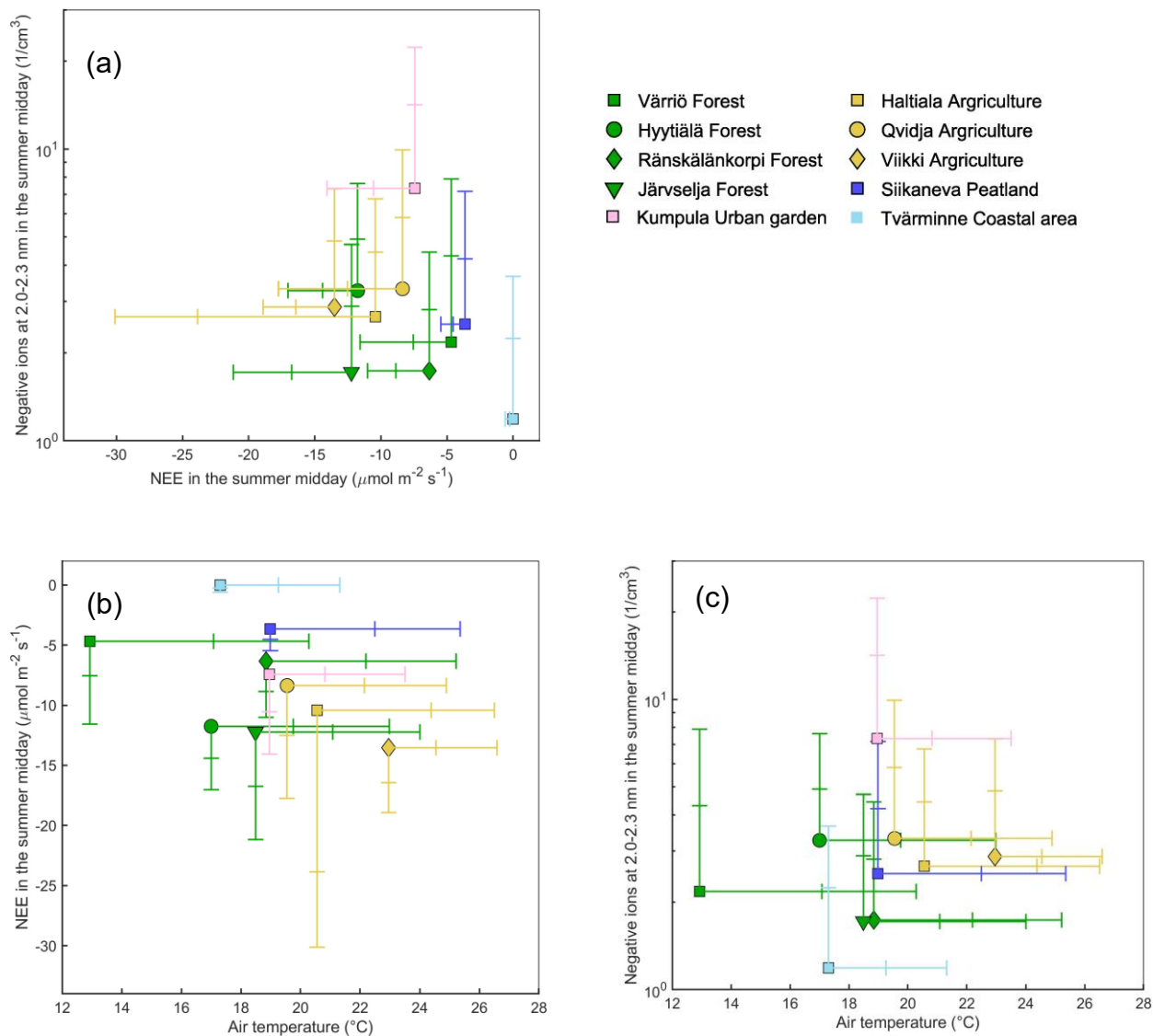
The variation of momentary NEE and  $N_{\text{neg}}$  were distinct even between a similar type of  
405 ecosystem in a similar latitude (Section 3.1 and 3.2), e.g., within forests and agricultural fields.  
For forests, the most southern F-JAR had the highest net CO<sub>2</sub> uptake rate, while the median  
 $N_{\text{neg}}$  in the midday in summer was similar to F-RAN and 53% of that in F-HYY. F-HYY had  
higher  $N_{\text{neg}}$  than the other forests. For agricultural sites, the net CO<sub>2</sub> uptake rate at A-VII and  
A-HAL were close to that in F-HYY, while it was 30% lower in A-QVI than in F-HYY. On  
410 the contrary, the  $N_{\text{neg}}$  were highest in A-QVI between the three agricultural sites, and median  
 $N_{\text{neg}}$  in the other two croplands were 12-19% smaller than in F-HYY.

Multiple factors can cause the difference in NEE and  $N_{\text{neg}}$  across the sites despite the similar  
seasonal and diurnal variation patterns. The CO<sub>2</sub> uptake rate at midday in summer increased  
with an increasing air temperature in both studied forests and agricultural fields (Figure 9).  
415 Moreover, the CO<sub>2</sub> uptake rate at midday in summer increased with LAI across the studied  
forest ecosystems (Table 1 and Figure S9). As F-RAN was selectively harvested (Section 2.3),  
the leaf area was decreased, which can result in a lower CO<sub>2</sub> uptake rate than other forests  
under similar air temperature and PPFD. Additionally, the peat soil at F-JAR and F-RAN can  
induce higher respiration (Figure 2). Hence, even though the LAI and air temperature at F-JAR  
420 were 23% and 10% higher than that in F-HYY, respectively, the NEE at F-JAR was only 4%  
lower than that at F-HYY. In the agricultural fields, the LAI and air temperature were  
comparable or higher than that in the forests, which may explain the high momentary CO<sub>2</sub>  
uptake rate at summer midday in the agricultural fields.

In the case of  $N_{\text{neg}}$ , the precursor of aerosol production largely influences  $N_{\text{neg}}$ . The trends of  
425  $N_{\text{neg}}$  varying with air temperature and radiation were not evident (Figures 9 and S9). H<sub>2</sub>SO<sub>4</sub>  
formation can drive the nucleation process and is influenced by the sulphur dioxide  
concentration and radiation. As the garden area and agricultural fields in this study are located  
in or nearby cities, the SO<sub>2</sub> concentration there may be enhanced due to the anthropogenic  
pollution and its long-range transport. Also, the terpene emissions can initiate NPF, which has  
430 been observed in Siikaneva peatland and led to stronger NPF there than that in F-HYY  
(Junninen et al., 2022; Huang et al., 2024). However, these events were reported to occur  
mostly in the late evening. Different plant species can emit different types of BVOCs (Guenther

et al, 2012), e.g., monoterpenes are found dominant in coniferous forests and isoprene dominant in broadleaf forests. The oxidation products of monoterpenes can enhance aerosol formation and growth (Rose et al., 2018), while isoprene has been reported to inhibit new particle formation (Kiendler-Scharr et al., 2009). As birch species are mixed with coniferous species in F-JAR, the possibly higher isoprene emission than in the other three predominantly coniferous forests may partially explain the lower  $N_{\text{neg}}$  in F-JAR. Moreover, the enhanced  $\text{NH}_3$  in agricultural fields can play a synergistic role with both  $\text{H}_2\text{SO}_4$  and low volatile organic compounds in clustering (Dada et al., 2023), which may explain the generally high  $N_{\text{neg}}$  in the three studied agricultural fields.

Overall, our results showed that agricultural fields have highest potential to contribute to momentary  $\text{CO}_2$  uptake and aerosol formation, affected by their vegetation and management practises. However, carbon inputs from fertilization and removal through harvested biomass in agricultural fields, which were not considered in our study, can lead to net carbon emissions in the annual carbon budgets (Heimsch et al., 2021; and references therein). Moreover, forests are the dominant landscape in Finland, covering ~9 times the area of agricultural fields (Table 2). Considering their large area, boreal forests in Finland are very likely the largest contributor of climate cooling when considering the  $\text{CO}_2$  uptake and local new particle formation.



455

Figure 9. Comparison of net ecosystem exchange (NEE) and negative intermediate ions at 2.0-2.3 nm (a), NEE and air temperature (b), and negative intermediate ions at 2.0-2.3 nm and air temperature (c) across different sites. The dots represent median values during summer midday (10:00-14:00). Error bars indicate the 10th and 25th percentiles for NEE, and the 75th and 90th percentiles for negative intermediate ions and air temperature, reflecting the CO<sub>2</sub> uptake rate and aerosol formation under optimal conditions.

Table 2. Comparison of NEE and negative intermediate ions at 2.0-2.3 nm size range across the hemi-boreal and boreal ecosystems at midday (10:00-14:00) in summer. The errors for median  $N_{\text{neg}}$  and NEE are standard deviation of their values across all the available years.

Ecosystem	Site (site ID)	Area in Finland (ha)	Median $N_{\text{neg}}$ ( $1/\text{cm}^3$ )	Median $N_{\text{neg}}/\text{median } N_{\text{neg, F-HYY}}$	75 <sup>th</sup> percentile $N_{\text{neg}}/75^{\text{th}}$ percentile $N_{\text{neg, F-HYY}}$	Midday NEE ( $\mu\text{mol m}^{-2} \text{s}^{-1}$ )	Median NEE/ median $\text{NEE}_{\text{F-HYY}}$	25 <sup>th</sup> percentile NEE/ 25 <sup>th</sup> percentile $\text{NEE}_{\text{F-HYY}}$
Forest	Hyytiälä (F-HYY)		3.3±0.53	1	1	-11.8±1.3	1	1
	Värriö (F-VAR)	20.3 million <sup>a</sup>	2.2±0.13	0.67	0.87	-4.7±1.2	0.4	0.52
	Järveljä (F-JAR)		1.7±0.12	0.53	0.58	-12±3.0	1.03	1.15
Drained peatland forest	Ränskälänkorpi (F-RAN)	4.2 million <sup>a</sup>	1.7±0.18	0.53	0.57	-6.4±2.3	0.54	0.61
Agricultural field	Haltiala (A-HAL)		2.7±0.22	0.94	1.06	-10±15	1.66	1.88
	Qvidja (A-QVI)	2.3 million <sup>a</sup>	3.3±0.30	1.01	1.17	-8.4±3.9	0.71	0.86
	Viikki (A-VII)		2.9	0.88	0.97	-14	1.14	1.13
Open peatland	Siikaneva (P-SII)	0.21 million <sup>b</sup>	2.5±0.26	0.77	0.85	-3.6±0.87	0.31	0.31
Urban garden area	Kumpula (G-KUM)	-----	7.3±0.68	2.24	2.86	-7.4±2.2	0.63	0.73
Coastal area	Tvärminne (C-TVA)	-----	1.2±0.07	0.36	0.46	-0.01±0.22	0.00	0.02

<sup>a</sup> Natural Resources Institute Finland 2022; <sup>b</sup> The area of oligotrophic open fens (Turunen and Valpola 2020);

----- data not available

### 3.4 Research limitations

In our study, only 1 year of data were applied in the stations with newly established atmospheric measurement, i.e., A-VII, although the measurement is continuing. The inter-annual variation of NEE has been widely observed across sites, e.g., F-HYY (Neefjes et al., 2022) and A-QVI (Heimsch et al., 2021), possibly due to annual changes in temperature and precipitations. In the reported year in A-VII, the air temperature was higher than that during 2015-2020 (Finnish Meteorological Institute; Figure S8). Since a higher air temperature can simultaneously increase the respiration and photosynthesis in an ecosystem, the influence of increased air temperature on the net CO<sub>2</sub> flux, i.e., NEE, is quite site-specific. More observation years are needed to reduce the estimation errors of NEE. Compared with NEE, the inter-annual variation of  $N_{\text{neg}}$  at summer midday fluctuated in a small magnitude across years (Table 2). Hence the measured  $N_{\text{neg}}$  in the reported year can be relatively representative of the local aerosol production at the site. Moreover, the  $N_{\text{neg}}$  may originate from area (sub-1 km; Tuovinen et al., 2024) larger than the ecosystem coverage, e.g., the agricultural sites within a radius of 500 m, leading to unavoidable uncertainties to the result.

Another potent greenhouse gas, methane (CH<sub>4</sub>) can be emitted through microbial activities in anoxic conditions, e.g., peatlands and coastal areas (Mathijssen et al., 2022; Roth et al., 2023). Considering that CH<sub>4</sub> has a sustained-flux global warming potential 45 times of CO<sub>2</sub> over 100 years (Roth et al., 2023; and the reference therein), the net CO<sub>2</sub> equivalent emission of CH<sub>4</sub> is estimated 2.5-8.6 times of CO<sub>2</sub> uptake in P-SII (Mathijssen et al., 2022). CH<sub>4</sub> emissions may largely compensate the CO<sub>2</sub> uptake in open and non-ditched peatlands. Similarly, the emission of CH<sub>4</sub> from coastal environment around Baltic Sea may offset 28% of the CO<sub>2</sub> sink in macroalgae-dominated coastal area (Roth et al., 2023). For ions, the summertime midday median  $N_{\text{neg}}$  at P-SII was 77% of that in F-HYYs (Table 2). As the open peatland is surrounded by forest within 1 km, the negative ion at 2.0-2.3 nm may be influenced by nearby forests.

Additionally, the albedo varies between each ecosystem type due to variations in vegetation cover (Peräkylä et al., 2025). Our research focused on the potential of different ecosystems for momentary CO<sub>2</sub> uptake and local aerosol production, thus omitting the albedo impact. Further research is still needed to evaluate the total climate impacts at the ecosystem level, including other greenhouse gas emission/uptake, albedo, carbon input from fertilization (for agricultural fields), and biomass harvest.

#### 500 4. Conclusions

The CarbonSink+ potential concept was established recently and provides a direct comparison of local contribution to CO<sub>2</sub> uptake and aerosol formation at ecosystem scale. The value of negative intermediate ion concentration at 2.0-2.3 nm size range ( $N_{\text{neg}}$ ) was applied as an indicator of the corresponding contribution of each ecosystem to produce new aerosol particles which, after their subsequent growth to larger sizes, are able to cool the atmosphere in a regional scale. Following this concept, net ecosystem CO<sub>2</sub> exchange fluxes (NEE) and  $N_{\text{neg}}$  were analysed in ten hemi-boreal and boreal ecosystems in Finland and Estonia.

The results showed that the agricultural fields had similar or even 15% higher CO<sub>2</sub> uptake potential compared to F-HYY during the summer midday, possibly due to the high leaf area index and air temperature in the agricultural fields. A distinct CO<sub>2</sub> uptake in the urban garden at midday in summer was observed, resulting from the strong photosynthesis of vegetation inside. The uptake rate was 37% lower than that in F-HYY but ~2 times of that in the open peatland. The coastal area considered in this study remained a very small CO<sub>2</sub> sink during summertime. The differences in  $N_{\text{neg}}$  between the studied sites were not as large as those in NEE. Ubiquitous nighttime clustering was observed across the terrestrial ecosystems. At midday in summer,  $N_{\text{neg}}$  was highest in the urban garden, followed by the agricultural fields. The coastal area had the lowest  $N_{\text{neg}}$ . The forest sites generally had lower  $N_{\text{neg}}$  than the agricultural sites. In agricultural fields, the synergetic role of NH<sub>3</sub>, H<sub>2</sub>SO<sub>4</sub>, and low volatile organic compounds originating from BVOC oxidation may play a synergistic role in clustering and induce a high  $N_{\text{neg}}$  generally comparing with other ecosystem types. The  $N_{\text{neg}}$  in the open peatland was 23% lower than F-HYY but 14-46% higher than other studied forests. Note that the urban garden and agricultural sites in Helsinki might be more influenced by air pollution compared to the forests and open peatland that were receiving little anthropogenic interference and pollution. The agricultural fields present highest potential to contribute to momentary CO<sub>2</sub> uptake and aerosol formation. However, it should be noted that the carbon in fertilization input and harvested biomass in agricultural fields were not included in this study. Overall, considering the large area of forests in Finland and Estonia, the forests in total are the largest contributors to climate cooling in terms of their CO<sub>2</sub> uptake and local new particle formation.



### **Data availability**

530 Measurement data at the sites, including ions data, eddy covariance data and meteorological data, are available upon request from the corresponding author before the relevant databases are open to the public.

### **Author contributions**

ST, JL, and RT were responsible for the ion measurements. PS, AL, MP, AL, MK, HR, LH, 535 AV, IM, and SN were responsible for the eddy covariance measurement and analysed the raw data. MK designed the study. PKe, AL, PKo, TN, OP, EE, TK, JB, VMK, and MK analysed the data and interpreted the results. PKe prepared the first-draft paper. All authors contributed to discussion of the results and provided input for the paper.

### **Competing interests**

540 The authors declare no competing interests.

### **Acknowledgement**

We acknowledge the following projects: ACCC Flagship funded by the Academy of Finland grant number 337549 (UH) and 337552 (FMI), Academy professorship funded by the Academy of Finland (grant no. 302958), Academy of Finland projects no. 1325656, 311932, 334792, 316114, 325647, 545 325681, 339489, the Strategic Research Council (SRC) at the Academy of Finland (352431), Jane and Aatos Erkko Foundation, “Gigacity” project funded by Wihuri foundation, European Research Council (ERC) project ATM-GTP (742206), and European Union via Non-CO<sub>2</sub> Forcers and their Climate, Weather, Air Quality and Health Impacts (FOCI). This project has received funding from the European Union – NextGenerationEU instrument and is funded by the Research Council of Finland under grant 550 number 347782. University of Helsinki support via ACTRIS-HY is acknowledged. Support of the technical and scientific staff in all sites are acknowledged. For SMEAR Estonia we acknowledge the Estonian Research Council Grant PRG 1674, the Estonian Environmental Investment Centre (KIK) project number 18392 and the European Union’s Horizon 2020 Research and Innovation programme (grant agreement no. 871115) ACTRIS IMP. INAR research infrastructure (RI), ICOS RI, ACTRIS RI 555 and eLTER RI are gratefully acknowledged for the continuous ecosystem-atmosphere measurements used in this study.

## Reference

- Aalto, J., Anttila, V., Kolari, P., Korpela, I., Isotalo, A., Levula, J., Schiestl-Aalto, P., and Bäck, J.,  
Hyttiälä SMEAR II Forest year 2020 thinning tree and carbon inventory data [dataset].  
560 <https://doi.org/10.5281/zenodo.7639833>.
- Aliaga, D., Tuovinen, S., Zhang, T., Lampilahti, J., Li, X., Ahonen, L., Kokkonen, T., Nieminen, T.,  
Hakala, S., Paasonen, P., Bianchi, F., Worsnop, D., Kerminen, V.-M., and Kulmala, M.: Nanoparticle  
ranking analysis: determining new particle formation (NPF) event occurrence and intensity based on  
the concentration spectrum of formed (sub-5 nm) particles, *Aerosol. Res.*, 1, 81-92,  
565 <https://doi.org/10.5194/ar-1-81-2023>, 2023.
- Alekseychik, P., Korrensalo, A., Mammarella, I., Launiainen, S., Tuittila, E.-S., Korpela, I., and Vesala,  
T.: Carbon balance of a Finnish bog: temporal variability and limiting factors based on 6 years of eddy-  
covariance data, *Biogeosciences*, 18, 4681-4704, [https://doi.org/https://doi.org/10.5194/bg-18-4681-](https://doi.org/https://doi.org/10.5194/bg-18-4681-2021)  
2021, 2021.
- 570 Artaxo, P., Hansson, H.-C., Andreae, M. O., Bäck, J., Alves, E. G., Barbosa, H. M. J., Bender, F.,  
Bourtsoukidis, E., Carbone, S., Chi, J., Decesari, S., Després, V. R., Ditas, F., Ezhova, E., Fuzzi, S.,  
Hasselquist, N. J., Heintzenberg, J., Holanda, B. A., Guenther, A., Hakola, H., Heikkinen, L., Kerminen,  
V.-M., Kontkanen, J., Krejci, R., Kulmala, M., Lavric, J. V., De Leeuw, G., Lehtipalo, K., Machado, L.  
A. T., McFiggans, G., Franco, M. A. M., Meller, B. B., Morais, F. G., Mohr, C., Morgan, W., Nilsson,  
575 M. B., Peichl, M., Petäjä, T., Praß, M., Pöhlker, C., Pöhlker, M. L., Pöschl, U., Von Randow, C.,  
Riipinen, I., Rinne, J., Rizzo, L. V., Rosenfeld, D., Silva Dias, M. A. F., Sogacheva, L., Stier, P.,  
Swietlicki, E., Sörgel, M., Tunved, P., Virkkula, A., Wang, J., Weber, B., Yáñez-Serrano, A. M., Zieger,  
P., Mikhailov, E., Smith, J. N., and Kesselmeier, J.: Tropical and Boreal Forest – Atmosphere  
Interactions: A Review, *Tellus B Chem. Phys. Meteorol.*, 74, 24, <https://doi.org/10.16993/tellusb.34>,  
580 2022.
- Aubinet, M., Grelle, A., Ibrom, A., Rannik, Ü., Moncrieff, J., Foken, T., Kowalski, A. S., Martin, P. H.,  
Berbigier, P., Bernhofer, C., Clement, R., Elbers, J., Granier, A., Grünwald, T., Morgenstern, K.,  
Pilegaard, K., Rebmann, C., Snijders, W., Valentini, R., and Vesala, T., 1999. Estimates of the Annual  
Net Carbon and Water Exchange of Forests: The EUROFLUX Methodology, in: *Advances in*  
585 *Ecological Research*, edited by: Fitter, A. H., and Raffaelli, D. G., Academic Press, 113-175,  
[https://doi.org/10.1016/S0065-2504\(08\)60018-5](https://doi.org/10.1016/S0065-2504(08)60018-5), 1999.
- Bao, X. X., Zhou, W. Q., Xu, L. L., and Zheng, Z.: A meta-analysis on plant volatile organic compound  
emissions of different plant species and responses to environmental stress, *Environ. Pollut.*, 318,  
<https://doi.org/10.1016/j.envpol.2022.120886>, 2023.

- 590 Chang, J. F., Ciais, P., Gasser, T., Smith, P., Herrero, M., Havlik, P., Obersteiner, M., Guenet, B., Goll, D. S., Li, W., Naipal, V., Peng, S. S., Qiu, C. J., Tian, H. Q., Viovy, N., Yue, C., and Zhu, D.: Climate warming from managed grasslands cancels the cooling effect of carbon sinks in sparsely grazed and natural grasslands, *Nat. Commun.*, 12, <https://doi.org/10.1038/s41467-020-20406-7>, 2021.
- Chen, X., Kerminen, V.-M., Paatero, J., Paasonen, P., Manninen, H. E., Nieminen, T., Petäjä, T., and  
595 Kulmala, M.: How do air ions reflect variations in ionising radiation in the lower atmosphere in a boreal forest?, *Atmos. Chem. Phys.*, 16, 14297-14315, <https://doi.org/10.5194/acp-16-14297-2016>, 2016.
- Dada, L., Chellapermal, R., Buenrostro Mazon, S., Paasonen, P., Lampilahti, J., Manninen, H. E., Junninen, H., Petäjä, T., Kerminen, V. M., and Kulmala, M.: Refined classification and characterization of atmospheric new-particle formation events using air ions, *Atmos. Chem. Phys.*, 18, 17883-17893,  
600 <https://doi.org/10.5194/acp-18-17883-2018>, 2018.
- Dada, L., Okuljar, M., Shen, J., Olin, M., Heimsch, L., Wu, Y., Baalbaki, R., Lampimäki, M., Kankaanrinta, S., Herlin, I., Kalliokoski, J., Lohila, A., Petäjä, T., Dal Maso, M., Duplissy, J., Kerminen, V.-M., and Kulmala, M.: Synergistic role of sulfuric acid, ammonia and organics in particle formation over an agricultural land, *Environ. Sci. Atmos.*, <https://doi.org/10.1039/d3ea00065f>, 2023.
- 605 Ezhova, E., Ylivinkka, I., Kuusk, J., Komsaare, K., Vana, M., Krasnova, A., Noe, S., Arshinov, M., Belan, B., Park, S.-B., Lavrič, J. V., Heimann, M., Petäjä, T., Vesala, T., Mammarella, I., Kolari, P., Bäck, J., Rannik, Ü., Kerminen, V.-M., and Kulmala, M.: Direct effect of aerosols on solar radiation and gross primary production in boreal and hemiboreal forests, *Atmos. Chem. Phys.*, 18, 17863–17881, <https://doi.org/10.5194/acp-18-17863-2018>, 2018.
- 610 Finnish Meteorological Institute. Download observations. Available at: <https://en.ilmatieteenlaitos.fi/download-observations> (Accessed: [2024-02-26]).
- Foken, T. and Wichura, B.: Tools for quality assessment of surface-based flux measurements, *Agric. For. Meteorol.*, 78, 83-105, [https://doi.org/10.1016/0168-1923\(95\)02248-1](https://doi.org/10.1016/0168-1923(95)02248-1), 1996.
- Fratini, G. and Mauder, M.: Towards a consistent eddy-covariance processing: an intercomparison of  
615 EddyPro and TK3, *Atmos. Meas. Tech.*, 7, 2273-2281, <https://doi.org/10.5194/amt-7-2273-2014>, 2014.
- Friedlingstein, P., O'Sullivan, M., Jones, M. W., Andrew, R. M., Gregor, L., Hauck, J., Le Quéré, C., Luijkx, I. T., Olsen, A., Peters, G. P., Peters, W., Pongratz, J., Schwingshackl, C., Sitch, S., Canadell, J. G., Ciais, P., Jackson, R. B., Alin, S. R., Alkama, R., Arneth, A., Arora, V. K., Bates, N. R., Becker, M., Bellouin, N., Bittig, H. C., Bopp, L., Chevallier, F., Chini, L. P., Cronin, M., Evans, W., Falk, S.,  
620 Feely, R. A., Gasser, T., Gehlen, M., Gkritzalis, T., Gloege, L., Grassi, G., Gruber, N., Gürses, Ö., Harris, I., Hefner, M., Houghton, R. A., Hurtt, G. C., Iida, Y., Ilyina, T., Jain, A. K., Jersild, A., Kadono, K., Kato, E., Kennedy, D., Klein Goldewijk, K., Knauer, J., Korsbakken, J. I., Landschützer, P., Lefèvre, N., Lindsay, K., Liu, J., Liu, Z., Marland, G., Mayot, N., McGrath, M. J., Metzl, N., Monacchi, N. M.,

Munro, D. R., Nakaoka, S.-I., Niwa, Y., O'Brien, K., Ono, T., Palmer, P. I., Pan, N., Pierrot, D., Pocock, K., Poulter, B., Resplandy, L., Robertson, E., Rödenbeck, C., Rodriguez, C., Rosan, T. M., Schwinger, J., Séférian, R., Shutler, J. D., Skjelvan, I., Steinhoff, T., Sun, Q., Sutton, A. J., Sweeney, C., Takao, S., Tanhua, T., Tans, P. P., Tian, X., Tian, H., Tilbrook, B., Tsujino, H., Tubiello, F., Van Der Werf, G. R., Walker, A. P., Wanninkhof, R., Whitehead, C., Willstrand Wranne, A., Wright, R., Yuan, W., Yue, C., Yue, X., Zaehle, S., Zeng, J., and Zheng, B.: Global Carbon Budget 2022, *Earth Syst. Sci. Data*, 14, 4811-4900, <https://doi.org/10.5194/essd-14-4811-2022>, 2022.

Gordon, H., Kirkby, J., Baltensperger, U., Bianchi, F., Breitenlechner, M., Curtius, J., Dias, A., Dommen, J., Donahue, N. M., Dunne, E. M., Duplissy, J., Ehrhart, S., Flagan, R. C., Frege, C., Fuchs, C., Hansel, A., Hoyle, C. R., Kulmala, M., Kürten, A., Lehtipalo, K., Makhmutov, V., Molteni, U., Rissanen, M. P., Stozkhov, Y., Tröstl, J., Tsagkogeorgas, G., Wagner, R., Williamson, C., Wimmer, D., Winkler, P. M., Yan, C., and Carslaw, K. S.: Causes and importance of new particle formation in the present-day and preindustrial atmospheres, *J. Geophys. Res. Atmos.*, 122, 8739-8760, <https://doi.org/10.1002/2017JD026844>, 2017.

Guenther, A. B., Jiang, X., Heald, C. L., Sakulyanontvittaya, T., Duhl, T., Emmons, L. K., and Wang, X.: The Model of Emissions of Gases and Aerosols from Nature version 2.1 (MEGAN2.1): an extended and updated framework for modeling biogenic emissions, *Geosci. Model Dev.*, 5, 1471-1492, <https://doi.org/10.5194/gmd-5-1471-2012>, 2012.

Heimsch, L., Lohila, A., Tuovinen, J.-P., Vekuri, H., Heinonsalo, J., Nevalainen, O., Korkiakoski, M., Liski, J., Laurila, T., and Kulmala, L.: Carbon dioxide fluxes and carbon balance of an agricultural grassland in southern Finland, *Biogeosciences*, 18, 3467-3483, <https://doi.org/10.5194/bg-18-3467-2021>, 2021.

Huang, W., Junninen, H., Garmash, O., Lehtipalo, K., Stolzenburg, D., Lampilahti, J., Ezhova, E., Schallhart, S., Rantala, P., Aliaga, D., Ahonen, L., Sulo, J., Quéléver, L. L. J., Cai, R., Alekseychik, P., Mazon, S. B., Yao, L., M. Blichner, S., Zha, Q., Mammarella, I., Kirkby, J., Kerminen, V.-M., Worsnop, D. R., Kulmala, M., and Bianchi, F.: Potential pre-industrial-like new particle formation induced by pure biogenic organic vapors in Finnish peatland, *Sci. Adv.*, 10, eadm9191, <https://doi.org/10.1126/sciadv.adm9191>, 2024.

IPCC, 2022. Annex I: Glossary, in: *Global Warming of 1.5°C: IPCC Special Report on Impacts of Global Warming of 1.5°C above Pre-industrial Levels in Context of Strengthening Response to Climate Change, Sustainable Development, and Efforts to Eradicate Poverty*, edited by: Intergovernmental Panel on Climate, C., Cambridge University Press, Cambridge, 541-562, <https://doi.org/10.1017/9781009157940.008>, 2022.

- Järvi, L., Nordbo, A., Junninen, H., Riikonen, A., Moilanen, J., Nikinmaa, E., and Vesala, T.: Seasonal and annual variation of carbon dioxide surface fluxes in Helsinki, Finland, in 2006–2010, *Atmos. Chem. Phys.*, 12, 8475–8489, <https://doi.org/10.5194/acp-12-8475-2012>, 2012.
- 660 Jia, G., Shevliakova, E., Artaxo, P., Noblet-Ducoudré, N. D., Houghton, R., House, J., Kitajima, K., C. Lennard, Popp, A., A. Sirin, Sukumar, R., and Verchot, L., 2022. Land–climate interactions, in: *Climate Change and Land: IPCC Special Report on Climate Change, Desertification, Land Degradation, Sustainable Land Management, Food Security, and Greenhouse Gas Fluxes in Terrestrial Ecosystems*, edited by: Intergovernmental Panel on Climate, C., Cambridge University Press, Cambridge, 131–248, 665 <https://doi.org/10.1017/9781009157988.004>, 2022.
- Junninen, H., Ahonen, L., Bianchi, F., Quéléver, L., Schallhart, S., Dada, L., Manninen, H. E., Leino, K., Lampilahti, J., Buenrostro Mazon, S., Rantala, P., Rätty, M., Kontkanen, J., Negri, S., Aliaga, D., Garmash, O., Alekseychik, P., Lipp, H., Tamme, K., Levula, J., Sipilä, M., Ehn, M., Worsnop, D., Zilitinkevich, S., Mammarella, I., Rinne, J., Vesala, T., Petäjä, T., Kerminen, V.-M., and Kulmala, M.: 670 Terpene emissions from boreal wetlands can initiate stronger atmospheric new particle formation than boreal forests, *Commun. Earth Environ.*, 3, <https://doi.org/10.1038/s43247-022-00406-9>, 2022.
- Kammer, J., Simon, L., Ciuraru, R., Petit, J.-E., Lafouge, F., Buysse, P., Bsaibes, S., Henderson, B., Cristescu, S. M., Durand, B., Fanucci, O., Truong, F., Gros, V., and Loubet, B.: New particle formation at a peri-urban agricultural site, *Sci. Total Environ.*, 857, 159370, 675 <https://doi.org/10.1016/j.scitotenv.2022.159370>, 2023.
- Kangur, A., Nigul, K., Padari, A., Kiviste, A., Korjus, H., Laarmann, D., Pöldveer, E., Mitt, R., Frelich, L., Jõgiste, K., Stanturf, J., Paluots, T., Kängsepp, V., Jürgenson, H., Noe, S., Sims, A., and Metslaid, M.: Composition of live, dead and downed trees in Järvelja old-growth forest, *Forestry Studies / Metsanduslikud Uurimused*, 75, 15–40, <https://doi.org/10.2478/fsmu-2021-0009>, 2021.
- 680 Kerminen, V.-M., Chen, X., Vakkari, V., Petäjä, T., Kulmala, M., and Bianchi, F.: Atmospheric new particle formation and growth: review of field observations, *Environ. Res. Lett.*, 13, 103003, <https://doi.org/10.1088/1748-9326/aadf3c>, 2018.
- Kiendler-Scharr, A., Wildt, J., Maso, M. D., Hohaus, T., Kleist, E., Mentel, T. F., Tillmann, R., Uerlings, R., Schurr, U., and Wahner, A.: New particle formation in forests inhibited by isoprene emissions, 685 *Nature*, 461, 381–384, <https://doi.org/10.1038/nature08292>, 2009.
- Kulmala, M., Ezhova, E., Kalliokoski, T., Noe, S., Vesala, T., Lohila, A., Liski, J., Makkonen, R., Bäck, J., Petäjä, T., Kerminen, V.-M., and Kerminen, P.: CarbonSink+ -Accounting for multiple climate feedbacks from forests, *Boreal Environ. Res.*, 25, 145–159, 2020.
- Kulmala, M., Ke, P., Lintunen, A., Peräkylä, O., Lohtander, A., Tuovinen, S., Lampilahti, J., Kolari, P., 690 Schiestl-Aalto, P., Kokkonen, T., Nieminen, T., Dada, L., Ylivinkka, I., Petäjä, T., Bäck, J., Lohila, A.,

- Heimsch, L., Ezhova, E., and Kerminen, V.-M.: A novel concept for assessing the potential of different boreal ecosystems to mitigate climate change (CarbonSink+ Potential), *Boreal Environ. Res.*, 29, 2024.
- Mäki, M., Ryhti, K., Fer, I., Ľupek, B., Vestin, P., Roland, M., Lehner, I., Köster, E., Lehtonen, A., Bäck, J., Heinonsalo, J., Pumpanen, J., and Kulmala, L.: Heterotrophic and rhizospheric respiration in  
695 coniferous forest soils along a latitudinal gradient, *Agricultural and Forest Meteorology*, 317, 108876, <https://doi.org/https://doi.org/10.1016/j.agrformet.2022.108876>, 2022.
- Kulmala, M., Nieminen, T., Nikandrova, A., Lehtipalo, K., Manninen, H., Kajos, M., Kolari, P., Lauri, A., Petaja, T., Krejci, R., Hansson, H.-C., Swietlicki, E., Lindroth, A., Christensen, T. R., Arneth, A., Hari, P., Back, J., Vesala, T., and Kerminen, V.-M.: CO<sub>2</sub>-induced terrestrial climate feedback  
700 mechanism: from carbon sink to aerosol source and back, *Boreal Environ. Res.*, 19, 122-131, 2014.
- Kulmala, L., Pumpanen, J., Kolari, P., Dengel, S., Berninger, F., Köster, K., Matkala, L., Vanhatalo, A., Vesala, T., and Bäck, J.: Inter- and intra-annual dynamics of photosynthesis differ between forest floor vegetation and tree canopy in a subarctic Scots pine stand, *Agric. For. Meteorol.*, 271, 1-11, <https://doi.org/10.1016/j.agrformet.2019.02.029>, 2019.
- 705 Kulmala, M., Suni, T., Lehtinen, K. E. J., Dal Maso, M., Boy, M., Reissell, A., Rannik, Ü., Aalto, P., Keronen, P., Hakola, H., Bäck, J., Hoffmann, T., Vesala, T., and Hari, P.: A new feedback mechanism linking forests, aerosols, and climate, *Atmos. Chem. Phys.*, 4, 557-562, <https://doi.org/10.5194/acp-4-557-2004>, 2004.
- Laurila, T., Aurela, M., Hatakka, J., Hotanen, J.-P., Jauhiainen, J., Korkiakoski, M., Korpela, L.,  
710 Koskinen, M., Laiho, R., Lehtonen, A., Alder, K., Linkosalmi, M., Salmon, A., Minkkinen, K., Mäkelä, T., Mäkiranta, P., Nieminen, M., Ojanen, P., Peltoniemi, M., Penttilä, T., Rainne, J., Rautakoski, H., Saarinen, M., Salovaara, P., Sarkkola, S., and Mäkipää, R. : Set-up and instrumentation of the greenhouse gas (GHG) measurements on experimental sites of continuous cover forestry, *Natural Resources and Bioeconomy Studies*, 26, 2021.
- 715 Lee, X. and Hu, X.: Forest-air fluxes of carbon, water and energy over non-flat terrain, *Bound.-Layer Meteorol.*, 103, 277-301, <https://doi.org/10.1023/A:1014508928693>, 2002.
- Lehtipalo, K., Yan, C., Dada, L., Bianchi, F., Xiao, M., Wagner, R., Stolzenburg, D., Ahonen, L. R., Amorim, A., Baccarini, A., Bauer, P. S., Baumgartner, B., Bergen, A., Bernhammer, A.-K., Breitenlechner, M., Brilke, S., Buchholz, A., Mazon, S. B., Chen, D., Chen, X., Dias, A., Dommen, J.,  
720 Draper, D. C., Duplissy, J., Ehn, M., Finkenzeller, H., Fischer, L., Frege, C., Fuchs, C., Garmash, O., Gordon, H., Hakala, J., He, X., Heikkinen, L., Heinritzi, M., Helm, J. C., Hofbauer, V., Hoyle, C. R., Jokinen, T., Kangasluoma, J., Kerminen, V.-M., Kim, C., Kirkby, J., Kontkanen, J., Kürten, A., Lawler, M. J., Mai, H., Mathot, S., Mauldin, R. L., Molteni, U., Nichman, L., Nie, W., Nieminen, T., Ojdanic, A., Onnela, A., Passananti, M., Petäjä, T., Piel, F., Pospisilova, V., Quéléver, L. L. J., Rissanen, M. P.,

- 725 Rose, C., Sarnela, N., Schallhart, S., Schuchmann, S., Sengupta, K., Simon, M., Sipilä, M., Tauber, C.,  
Tomé, A., Tröstl, J., Väisänen, O., Vogel, A. L., Volkamer, R., Wagner, A. C., Wang, M., Weitz, L.,  
Wimmer, D., Ye, P., Ylisirniö, A., Zha, Q., Carslaw, K. S., Curtius, J., Donahue, N. M., Flagan, R. C.,  
Hansel, A., Riipinen, I., Virtanen, A., Winkler, P. M., Baltensperger, U., Kulmala, M., and Worsnop,  
730 D. R.: Multicomponent new particle formation from sulfuric acid, ammonia, and biogenic vapors, *Sci.*  
*Adv.*, 4, eaau5363, <https://doi.org/doi:10.1126/sciadv.aau5363>, 2018.
- Mammarella, I., Peltola, O., Nordbo, A., Järvi, L., and Rannik, Ü.: Quantifying the uncertainty of eddy  
covariance fluxes due to the use of different software packages and combinations of processing steps  
in two contrasting ecosystems, *Atmos. Meas. Tech.*, 9, 4915-4933, [https://doi.org/10.5194/amt-9-4915-](https://doi.org/10.5194/amt-9-4915-2016)  
2016, 2016.
- 735 Manninen, H. E., Mirme, S., Mirme, A., Petäjä, T., and Kulmala, M.: How to reliably detect molecular  
clusters and nucleation mode particles with Neutral cluster and Air Ion Spectrometer (NAIS), *Atmos.*  
*Meas. Tech.*, 9, 3577-3605, <https://doi.org/10.5194/amt-9-3577-2016>, 2016.
- Mathijssen, P. J. H., Tuovinen, J. P., Lohila, A., Välranta, M., and Tuittila, E. S.: Identifying main  
uncertainties in estimating past and present radiative forcing of peatlands, *Glob. Chang. Biol.*, 28, 4069-  
740 4084, <https://doi.org/10.1111/gcb.16189>, 2022.
- Mazon, S. B., Kontkanen, J., Manninen, H. E., Nieminen, T., Kerminen, V. M., and Kulmala, M.: A  
long-term comparison of nighttime cluster events and daytime ion formation in a boreal forest, *Boreal*  
*Environ. Res.*, 21, 242-261, 2016.
- Mirme S. and Mirme A.: The mathematical principles and design of the NAIS — a spectrometer for the  
745 measurement of cluster ion and nanometer aerosol size distributions. *Atmos. Meas. Tech.* 6: 1061-1071,  
2013.
- Natural Resources Institute Finland 2022. <https://www.luke.fi/en/statistics>, last access: 2023, 07.
- Neefjes, I., Laapas, M., Médus, E., Meittunen, E., Ahonen, L., Quéléver, L., Aaltio, J., Bäck, J.,  
Kerminen, V.-M., Lampilahti, J., Luoma, K., Maki, M., Mammarella, I., Petäjä, T., Rätty, M., Sarnela,  
750 N., Ylivinkka, I., Hakala, S., Kulmala, M., and Liu, Y.: 25 years of atmospheric and ecosystem  
measurements in a boreal forest — Seasonal variation and responses to warm and dry years, *Boreal*  
*Environ. Res.*, 27, 1-31, 2022.
- Nieminen, T., Kerminen, V.-M., Petäjä, T., Aalto, P. P., Arshinov, M., Asmi, E., Baltensperger, U.,  
Beddows, D. C. S., Beukes, J. P., Collins, D., Ding, A., Harrison, R. M., Henzing, B., Hooda, R., Hu,  
755 M., Hörrak, U., Kivekäs, N., Komsaare, K., Krejci, R., Kristensson, A., Laakso, L., Laaksonen, A.,  
Leaich, W. R., Lihavainen, H., Mihalopoulos, N., Németh, Z., Nie, W., O'Dowd, C., Salma, I., Sellegri,  
K., Svenningsson, B., Swietlicki, E., Tunved, P., Ulevicius, V., Vakkari, V., Vana, M., Wiedensohler,  
A., Wu, Z., Virtanen, A., and Kulmala, M.: Global analysis of continental boundary layer new particle

- formation based on long-term measurements, *Atmos. Chem. Phys.*, 18, 14737-14756, <https://doi.org/10.5194/acp-18-14737-2018>, 2018.
- Noe, S., Niinemets, Ü., Krasnova, A., Krasnov, D., Motallebi, A., Kängsepp, V., Jõgiste, K., Hörrak, U., Komsaare, K., Mirme, S., Vana, M., Tammet, H., Bäck, J., Vesala, T., Kulmala, M., Petäjä, T., and Kangur, A.: SMEAR Estonia: Perspectives of a large-scale forest ecosystem– Atmosphere research infrastructure, *For. Stud.*, 63, 56-84, <https://doi.org/10.1515/fsmu-2015-0009>, 2015.
- Olin, M., Okuljar, M., Rissanen, M. P., Kalliokoski, J., Shen, J., Dada, L., Lampimäki, M., Wu, Y., Lohila, A., Duplissy, J., Sipilä, M., Petäjä, T., Kulmala, M., and Dal Maso, M.: Measurement report: Atmospheric new particle formation in a coastal agricultural site explained with binPMF analysis of nitrate CI-API-TOF spectra, *Atmos. Chem. Phys.*, 22, 8097-8115, <https://doi.org/10.5194/acp-22-8097-2022>, 2022.
- Peräkylä, O., Rinne, E., Ezhova, E., Lintunen, A., Lohila, A., Aalto, J., Aurela, M., Kolari, P., and Kulmala, M.: Comparison of shortwave radiation dynamics between boreal forest and open peatland pairs in southern and northern Finland, *Biogeosciences*, 22, 153-179, <https://doi.org/10.5194/bg-22-153-2025>, 2025.
- Petäjä, T., Tabakova, K., Manninen, A., Ezhova, E., O'Connor, E., Moiseev, D., Sinclair, V. A., Backman, J., Levula, J., Luoma, K., Virkkula, A., Paramonov, M., Rätty, M., Äijälä, M., Heikkinen, L., Ehn, M., Sipilä, M., Yli-Juuti, T., Virtanen, A., Ritsche, M., Hickmon, N., Pulik, G., Rosenfeld, D., Worsnop, D. R., Bäck, J., Kulmala, M., and Kerminen, V. M.: Influence of biogenic emissions from boreal forests on aerosol–cloud interactions, *Nat. Geosci.*, 15, 42-47, <https://doi.org/10.1038/s41561-021-00876-0>, 2022.
- Rätty, M., Sogacheva, L., Keskinen, H. M., Kerminen, V. M., Nieminen, T., Petäjä, T., Ezhova, E., and Kulmala, M.: Dynamics of aerosol, humidity, and clouds in air masses travelling over Fennoscandian boreal forests, *Atmos. Chem. Phys.*, 23, 3779-3798, <https://doi.org/10.5194/acp-23-3779-2023>, 2023.
- Regnier, P., Resplandy, L., Najjar, R. G., and Ciais, P.: The land-to-ocean loops of the global carbon cycle, *Nature*, 603, 401-410, <https://doi.org/10.1038/s41586-021-04339-9>, 2022.
- Rinne, J., Tuittila, E.-S., Peltola, O., Li, X., Raivonen, M., Alekseychik, P., Haapanala, S., Pihlatie, M., Aurela, M., Mammarella, I., and Vesala, T.: Temporal Variation of Ecosystem Scale Methane Emission From a Boreal Fen in Relation to Temperature, Water Table Position, and Carbon Dioxide Fluxes, *Global Biogeochem Cy.*, 32, 1087-1106, <https://doi.org/10.1029/2017gb005747>, 2018.
- Rose, C., Zha, Q., Dada, L., Yan, C., Lehtipalo, K., Junninen, H., Mazon, S. B., Jokinen, T., Sarnela, N., Sipilä, M., Petäjä, T., Kerminen, V.-M., Bianchi, F., and Kulmala, M.: Observations of biogenic ion-induced cluster formation in the atmosphere, *Science Advances*, 4, eaar5218, <https://doi.org/doi:10.1126/sciadv.aar5218>, 2018.



- Rosenfeld, D., Andreae, M. O., Asmi, A., Chin, M., De Leeuw, G., Donovan, D. P., Kahn, R., Kinne, S., Kivekäs, N., Kulmala, M., Lau, W., Schmidt, K. S., Suni, T., Wagner, T., Wild, M., and Quaas, J.:  
795 Global observations of aerosol-cloud-precipitation-climate interactions, *Rev. Geophys.*, 52, 750-808,  
<https://doi.org/10.1002/2013rg000441>, 2014.
- Roth, F., Broman, E., Sun, X., Bonaglia, S., Nascimento, F., Prytherch, J., Brüchert, V., Lundevall Zara, M., Brunberg, M., Geibel, M. C., Humborg, C., and Norkko, A.: Methane emissions offset atmospheric  
800 carbon dioxide uptake in coastal macroalgae, mixed vegetation and sediment ecosystems, *Nat. Commun.*,  
14, <https://doi.org/10.1038/s41467-022-35673-9>, 2023.
- Stolzenburg, D., Cai, R., Blichner, S. M., Kontkanen, J., Zhou, P., Makkonen, R., Kerminen, V.-M.,  
Kulmala, M., Riipinen, I., and Kangasluoma, J.: Atmospheric nanoparticle growth, *Rev. Mod. Phys.*,  
95, 045002, <https://doi.org/10.1103/RevModPhys.95.045002>, 2023.
- Tammet, H., Komsaare, K., and Hörrak, U.: Intermediate ions in the atmosphere, *Atmos. Res.*, 135-136,  
805 263-273, <https://doi.org/10.1016/j.atmosres.2012.09.009>, 2014.
- Turunen, J., Valpola, S.: The influence of anthropogenic land use on Finnish peatland area and carbon  
stores 1950–2015, *Mires and Peat*, 26, 26, 27pp, <https://doi.org/10.19189/MaP.2019.GDC.StA.1870>,  
2022. (Online: <http://www.mires-and-peat.net/pages/volumes/map26/map2626.php>).
- Virtasalo, J. J., Österholm, P., and Asmala, E.: Estuarine flocculation dynamics of organic carbon and  
810 metals from boreal acid sulfate soils. *Biogeosciences*, 20(14), 2883-2901. <https://doi.org/10.5194/bg-20-2883-2023>, 2023.
- Tuovinen, S., Lampilahti, J., Kerminen, V.-M., and Kulmala, M.: Intermediate ions as indicator for  
local new particle formation, *Aerosol. Res.* [preprint], <https://doi.org/10.5194/ar-2024-4>, in review,  
2024.
- 815 Walker, A. P., De Kauwe, M. G., Bastos, A., Belmecheri, S., Georgiou, K., Keeling, R. F., McMahon,  
S. M., Medlyn, B. E., Moore, D. J. P., Norby, R. J., Zaehle, S., Anderson-Teixeira, K. J., Battipaglia,  
G., Brien, R. J. W., Cabugao, K. G., Cailleret, M., Campbell, E., Canadell, J. G., Ciais, P., Craig, M.  
E., Ellsworth, D. S., Farquhar, G. D., Fatichi, S., Fisher, J. B., Frank, D. C., Graven, H., Gu, L., Haverd,  
V., Heilman, K., Heimann, M., Hungate, B. A., Iversen, C. M., Joos, F., Jiang, M., Keenan, T. F.,  
820 Knauer, J., Körner, C., Leshyk, V. O., Leuzinger, S., Liu, Y., Macbean, N., Malhi, Y., McVicar, T. R.,  
Penuelas, J., Pongratz, J., Powell, A. S., Riutta, T., Sabot, M. E. B., Schleucher, J., Sitch, S., Smith, W.  
K., Sulman, B., Taylor, B., Terrer, C., Torn, M. S., Treseder, K. K., Trugman, A. T., Trumbore, S. E.,  
Van Mantgem, P. J., Voelker, S. L., Whelan, M. E., and Zuidema, P. A.: Integrating the evidence for a  
terrestrial carbon sink caused by increasing atmospheric CO<sub>2</sub>, *New Phytol.*, 229, 2413-2445,  
825 <https://doi.org/10.1111/nph.16866>, 2021.
- Yi, C. X., Ricciuto, D., Li, R., Wolbeck, J., Xu, X. Y., Nilsson, M., Aires, L., Albertson, J. D., Ammann,  
C., Arain, M. A., de Araujo, A. C., Aubinet, M., Aurela, M., Barcza, Z., Barr, A., Berbigier, P., Beringer,

- J., Bernhofer, C., Black, A. T., Bolstad, P. V., Bosveld, F. C., Broadmeadow, M. S. J., Buchmann, N., Burns, S. P., Cellier, P., Chen, J. M., Chen, J. Q., Ciais, P., Clement, R., Cook, B. D., Curtis, P. S., Dail, 830 D. B., Dellwik, E., Delpierre, N., Desai, A. R., Dore, S., Dragoni, D., Drake, B. G., Dufrene, E., Dunn, A., Elbers, J., Eugster, W., Falk, M., Feigenwinter, C., Flanagan, L. B., Foken, T., Frank, J., Fuhrer, J., Gianelle, D., Goldstein, A., Goulden, M., Granier, A., Grünwald, T., Gu, L., Guo, H. Q., Hammerle, A., Han, S. J., Hanan, N. P., Haszpra, L., Heinesch, B., Helfter, C., Hendriks, D., Hutley, L. B., Ibrom, A., Jacobs, C., Johansson, T., Jongen, M., Katul, G., Kiely, G., Klumpp, K., Knohl, A., Kolb, T., Kutsch, 835 W. L., Lafleur, P., Laurila, T., Leuning, R., Lindroth, A., Liu, H. P., Loubet, B., Manca, G., Marek, M., Margolis, H. A., Martin, T. A., Massman, W. J., Matamala, R., Matteucci, G., McCaughey, H., Merbold, L., Meyers, T., Migliavacca, M., Miglietta, F., Misson, L., Moelder, M., Moncrieff, J., Monson, R. K., Montagnani, L., Montes-Helu, M., Moors, E., Moureaux, C., Mukelabai, M. M., Munger, J. W., Myklebust, M., Nagy, Z., Noormets, A., Oechel, W., Oren, R., Pallardy, S. G., Kyaw, T. P. U., Pereira, 840 J. S., Pilegaard, K., Pintér, K., Pio, C., Pita, G., Powell, T. L., Rambal, S., Randerson, J. T., von Randow, C., Rebmann, C., Rinne, J., Rossi, F., Roulet, N., Ryel, R. J., Sagerfors, J., Saigusa, N., Sanz, M. J., Mugnozza, G. S., Schmid, H. P., Seufert, G., Siqueira, M., Soussana, J. F., Starr, G., Sutton, M. A., Tenhunen, J., Tuba, Z., Tuovinen, J. P., Valentini, R., Vogel, C. S., Wang, J. X., Wang, S. Q., Wang, W. G., Welp, L. R., Wen, X. F., Wharton, S., Wilkinson, M., Williams, C. A., Wohlfahrt, G., Yamamoto, 845 S., Yu, G. R., Zampedri, R., Zhao, B., and Zhao, X. Q.: Climate control of terrestrial carbon exchange across biomes and continents, *Environ. Res. Lett.*, 5, <https://doi.org/10.1088/1748-9326/5/3/034007>, 2010.
- Yli-Juuti, T., Mielonen, T., Heikkinen, L., Arola, A., Ehn, M., Isokääntä, S., Keskinen, H.-M., Kulmala, M., Laakso, A., Lipponen, A., Luoma, K., Mikkonen, S., Nieminen, T., Paasonen, P., Petäjä, T., 850 Romakkaniemi, S., Tonttila, J., Kokkola, H., and Virtanen, A.: Significance of the organic aerosol driven climate feedback in the boreal area, *Nat. Commun.*, 12, <https://doi.org/10.1038/s41467-021-25850-7>, 2021.
- Zhang, C., Hai, S., Gao, Y., Wang, Y., Zhang, S., Sheng, L., Zhao, B., Wang, S., Jiang, J., Huang, X., Shen, X., Sun, J., Lupascu, A., Shrivastava, M., Fast, J. D., Cheng, W., Guo, X., Chu, M., Ma, N., Hong, 855 J., Wang, Q., Yao, X., and Gao, H.: Substantially positive contributions of new particle formation to cloud condensation nuclei under low supersaturation in China based on numerical model improvements, *Atmos. Chem. Phys.*, 23, 10713-10730, <https://doi.org/10.5194/acp-23-10713-2023>, 2023.
- Zheng, G., Wang, Y., Wood, R., Jensen, M. P., Kuang, C., McCoy, I. L., Matthews, A., Mei, F., Tomlinson, J. M., Shilling, J. E., Zawadowicz, M. A., Crosbie, E., Moore, R., Ziemba, L., Andreae, M. 860 O., and Wang, J.: New particle formation in the remote marine boundary layer, *Nat. Commun.*, 12, <https://doi.org/10.1038/s41467-020-20773-1>, 2021.